

## Tbx3 Controls Dppa3 Levels and Exit from Pluripotency toward Mesoderm

Avinash Waghray,<sup>1,4</sup> Néstor Saiz,<sup>7</sup> Anitha D. Jayaprakash,<sup>4,6,8</sup> Ana G. Freire,<sup>1,2,3</sup> Dmitri Papatsenko,<sup>1</sup> Carlos-Filipe Pereira,<sup>1</sup> Dung-Fang Lee,<sup>1</sup> Ran Brosh,<sup>1</sup> Betty Chang,<sup>1,4</sup> Henia Darr,<sup>1</sup> Julian Gingold,<sup>1</sup> Kevin Kelley,<sup>1</sup> Christoph Schaniel,<sup>1,4,5</sup> Anna-Katerina Hadjantonakis,<sup>7</sup> and Ihor R. Lemischka<sup>1,4,5,\*</sup>

<sup>1</sup>Developmental and Regenerative Biology, The Black Family Stem Cell Institute, Icahn School of Medicine at Mount Sinai, New York, NY 10029, USA

<sup>2</sup>ICS - Instituto de Investigação e Inovação em Saúde & INEB - Instituto de Engenharia Biomédica, Universidade do Porto, 4150-180 Porto, Portugal

<sup>3</sup>Faculdade de Engenharia da Universidade do Porto, 4200-465 Porto, Portugal

<sup>4</sup>Graduate School, Icahn School of Medicine at Mount Sinai, New York, NY 10029, USA

<sup>5</sup>Pharmacology and System Therapeutics, Icahn School of Medicine at Mount Sinai, New York, NY 10029, USA

<sup>6</sup>Genetics and Genomic Sciences, Icahn School of Medicine at Mount Sinai, New York, NY 10029, USA

<sup>7</sup>Developmental Biology Program, Sloan Kettering Institute, Memorial Sloan Kettering Cancer Center, New York, NY 10029, USA

<sup>8</sup>Present address: Girihlet Inc., 423 West 127th Street, New York, NY 10027, USA

\*Correspondence: [ihor.lemischka@mssm.edu](mailto:ihor.lemischka@mssm.edu)

<http://dx.doi.org/10.1016/j.stemcr.2015.05.009>

This is an open access article under the CC BY-NC-ND license (<http://creativecommons.org/licenses/by-nc-nd/4.0/>).

## SUMMARY

Tbx3, a member of the T-box family, plays important roles in development, stem cells, nuclear reprogramming, and cancer. Loss of Tbx3 induces differentiation in mouse embryonic stem cells (mESCs). However, we show that mESCs exist in an alternate stable pluripotent state in the absence of Tbx3. In-depth transcriptome analysis of this mESC state reveals Dppa3 as a direct downstream target of Tbx3. Also, Tbx3 facilitates the cell fate transition from pluripotent cells to mesoderm progenitors by directly repressing Wnt pathway members required for differentiation. Wnt signaling regulates differentiation of mESCs into mesoderm progenitors and helps to maintain a naive pluripotent state. We show that Tbx3, a downstream target of Wnt signaling, fine tunes these divergent roles of Wnt signaling in mESCs. In conclusion, we identify a signaling-TF axis that controls the exit of mESCs from a self-renewing pluripotent state toward mesoderm differentiation.

## INTRODUCTION

Mouse embryonic stem cells (mESCs) are cells derived from inner cell mass (ICM) that self-renew indefinitely in culture and can give rise to all somatic cell types both in vitro and in vivo (Evans and Kaufman, 1981; Martin, 1981; Murry and Keller, 2008). The balance between self-renewal and differentiation is maintained by a milieu of transcription factors (TFs) (Ivanova et al., 2006; Thomson et al., 2011), epigenetic modifiers (Ang et al., 2011; Liang and Zhang, 2013; Loh et al., 2007), and signaling cascades (Lee et al., 2012a; Niwa et al., 2009). Many ESC-specific TFs such as Nanog (Chambers et al., 2007), Rex1 (Toyooka et al., 2008), Klf4 (Niwa et al., 2009; Toyooka et al., 2008), and Tbx3 (Niwa et al., 2009) are heterogeneously expressed in a population of mESCs (Faddah et al., 2013; MacArthur et al., 2012). These factors display low and high protein expression levels (Chambers et al., 2007; Toyooka et al., 2008). In the absence of some of these TFs (like Nanog), mESCs can maintain self-renewal and pluripotency (Chambers et al., 2007).

Expression of TFs like Nanog, Sox2, Esrrb, Klf4, and Tbx3 is controlled by external signaling cues (Niwa et al., 2009). Wnt signaling pathway has been widely studied in development (Nusse and Varmus, 2012), plays important roles in maintaining pluripotency (ten Berge et al., 2011; Ying et al., 2008), and is important for acquisition of pluripotency during induced pluripotent stem cell (iPSC) reprog-

ramming (Ho et al., 2013; Marson et al., 2008a). Downstream of Wnt ligand/receptor binding, the inhibition of GSK3 $\beta$  is necessary for stabilization of  $\beta$ -CATENIN (Nusse and Varmus, 2012). Inhibition of GSK3 $\beta$  and Mapk signaling with small molecules maintains a naive pluripotent state in mESCs (Sato et al., 2004; Ying et al., 2008). Wnt signaling stabilizes the mESC state in limiting amounts of LIF (Ogawa et al., 2006). Wnt3a prevents mESC differentiation from a naive to an epiblast-like or primed state (ten Berge et al., 2011). Apart from its role in maintenance of pluripotency, Wnt signaling is also required for differentiation of mESCs into early mesoderm derivatives (Gadue et al., 2006). Specifically, Wnt3 and Wnt8a are necessary for mesoderm differentiation (Kemp et al., 2005; Lindsley et al., 2006). During in vivo development, Wnt signaling is required for formation of primitive streak and mesoderm (Arnold et al., 2000; Martin and Kimelman, 2010; Yamaguchi et al., 1999). In summary, Wnt signaling is required both for stabilization of an undifferentiated pluripotent state and for promoting early mesoderm differentiation.

Expression of Tbx3 is regulated by Wnt signaling in mESCs (Kelly et al., 2011; Price et al., 2013) and cancer (Renard et al., 2007). Tbx3, the only member of its subfamily expressed in the ICM, is required for maintenance of ESC state (Chapman et al., 1996; Han et al., 2010; Ivanova et al., 2006). Tbx3 maintains self-renewal of mESCs in absence of LIF, a property shared by Nanog and Klf4



(Han et al., 2010). Tbx3 overexpressed with Oct4, Sox2, and Klf4 during iPSC-reprogramming improves germline competence of fully reprogrammed iPSCs (Han et al., 2010). Tbx3 overexpression also improves the efficiency of cell fusion-based reprogramming (Han et al., 2010). However, in vivo, Tbx3 null embryos survive until E10.5 (Davenport et al., 2003), beyond the blastocyst stage.

Many ESC-specific TFs like Oct4, Nanog, Sox2 (Mendjan et al., 2014; Thomson et al., 2011), and Sall4 (Lim et al., 2008) play important roles during early differentiation in addition to their roles in repressing differentiation of ESCs (Loh and Lim, 2011). Tbx3 promotes the formation of the mesendoderm lineage and is expressed both in ESCs and in vivo during primitive streak formation (Kartikasari et al., 2013; Weidgang et al., 2013). Furthermore, Tbx3 is required for generation of extraembryonic endoderm cells (Lu et al. 2011; Rugg-Gunn et al., 2010) and for opening up of *Eomes* promoter during differentiation to definitive endoderm (Kartikasari et al., 2013). However, the mechanisms by which Tbx3 regulates transition from a stable pluripotent state into differentiated progenitors remain unclear. Here, we explore how Tbx3 modulates the response of extracellular signaling and maintains balance between mESC self-renewal and differentiation. We isolate an alternate and stable pluripotent state in the absence of Tbx3 and identify *Dppa3* (Stella/PGC7) as a direct downstream target of Tbx3. We present a model in which the Wnt/Tbx3/Dppa3 signaling-TF axis controls specification of mESCs into mesoderm lineage.

## RESULTS

### A Subpopulation of mESCs Maintains a Tbx3 Null Pluripotent State

Tbx3 plays an important role in the maintenance of the mESC self-renewal state (Han et al., 2010; Ivanova et al., 2006). Upon RNAi-mediated Tbx3 depletion, mESCs differentiate even in the presence of LIF (Ivanova et al., 2006). We used a genetic complementation “rescue” system to control the expression of Tbx3 in ESCs (Figure S1A). In this system, called Tbx3R, endogenous Tbx3 is depleted by a constitutively expressed short-hairpin (sh) RNA and replaced with an exogenous shRNA-immune Tbx3 cDNA under the control of Doxycycline (Dox) (Ivanova et al., 2006). Five days after knockdown of Tbx3 (–Dox), mESCs lose their characteristic ESC-like morphology and alkaline phosphatase (AP) staining (Figure S1B). During the 5-day time course, mESCs also downregulate expression of pluripotency genes and upregulate differentiation markers (Figure S1C). Interestingly, upon prolonged culture of Tbx3-depleted cells, rare colonies with an ESC-like morphology emerge in a population of differentiating cells

(Figure S1D). We picked and expanded three of these colonies (clones 15, 16, and 17) for weeks in the absence of Dox (Figure 1A, right). We also picked and expanded some colonies grown in the presence of Dox (clones 27, 28, and 29) as controls (Figure 1A, left). All of the six clones maintained ESC-like morphology and AP activity (Figure 1A). *Tbx3* mRNA level was reduced in colonies without Dox, but they continued to express ESC markers such as *Oct4*, *Nanog*, *Sox2*, *Esrrb*, and *Tcl1* (Figure 1B). The level of TBX3 protein was reduced in colonies without Dox (Figures 1C and 1D), but they continued to express OCT4 and SOX2 proteins (Figure 1D). Tbx3 mRNA and protein is heterogeneously expressed in populations of mESCs (Kumar et al., 2014; MacArthur et al., 2012; Niwa et al., 2009). We confirmed these results by analyzing the expression of *Tbx3* mRNA in single mESCs discussed later. We therefore postulated that Tbx3 function might be dispensable in a subpopulation of mESCs upon long-term culture.

To explore this, we generated Tbx3 null mESCs from Tbx3 heterozygous ( $Tbx3^{+/N}$ ) mESCs (Davenport et al., 2003) using two approaches. First,  $Tbx3^{N/N}$  cells were generated via homologous recombination by culturing  $Tbx3^{+/N}$  cells in high concentrations of G418 (Figure S2A). Second,  $Tbx3^{N/P}$  cells were generated by targeting the WT allele in  $Tbx3^{+/N}$  cells (Figure S2A). We confirmed the targeted alleles by genomic PCR and Southern blotting (Figures S2B and 2C). Loss of TBX3 protein expression was confirmed (Figure S2D).  $Tbx3^{N/N}$  cells also maintained a normal karyotype in culture (Figure S2E). Both  $Tbx3^{N/P}$  and  $Tbx3^{N/N}$  cells maintain ESC-like morphology and AP activity (Figure 2A). Single  $Tbx3^{N/N}$  cells retain the ability to form AP-positive colonies with efficiencies equal to WT and  $Tbx3^{+/N}$  cells (Figure 2B). We tested the developmental potential of  $Tbx3^{N/N}$  and  $Tbx3^{N/P}$  mESCs using the blastocyst injection assay.  $Tbx3^{+/N}$  cells were used as control in the experiment. To mark ESCs and their descendants in chimeras,  $Tbx3^{+/N}$  and  $Tbx3^{N/P}$  cells were infected with lentiviral tdTomato vector, and  $Tbx3^{N/N}$  cells were infected with lentiviral eGFP vector. Both  $Tbx3^{N/N}$  and  $Tbx3^{N/P}$  cells extensively contributed to various tissues of E10.5 embryos indicated by expression of GFP or tdTomato throughout the chimeric embryos (Figure 2C; Table S6). It has also been reported that  $Tbx3^{N/N}$  embryos, derived by mating  $Tbx3^{+/N}$  mice, give rise to live embryos that survive without any apparent defects until E10.5, after which they exhibit a variety of defects in various tissues, including the yolk sac, limbs, and emergent mammary glands (Davenport et al., 2003). The mRNA expression levels of a selected panel of ESC genes also did not change significantly (>2-fold) between  $Tbx3^{+/+}$ ,  $Tbx3^{+/N}$ ,  $Tbx3^{N/N}$ , and  $Tbx3^{N/P}$  mESCs with the exception of *Dppa3*, which is discussed in detail later (Figure 2D). To further characterize Tbx3 null mESCs, we used a heterokaryon-based reprogramming

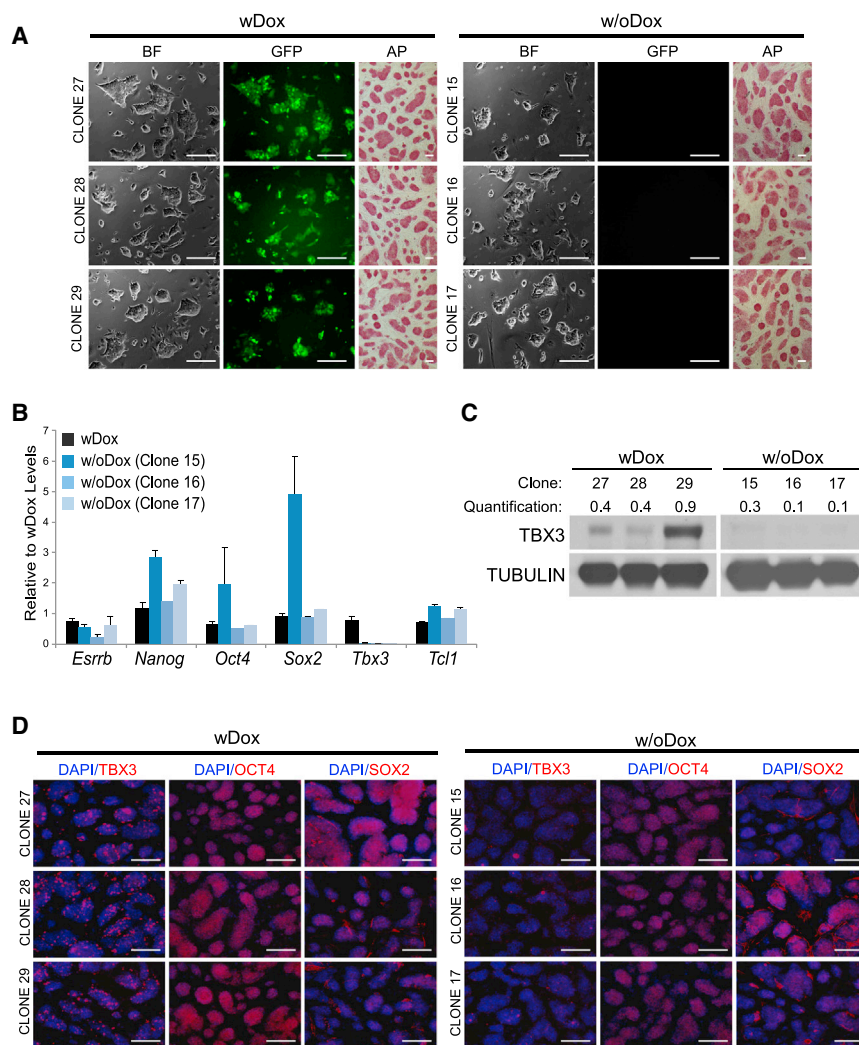


### Figure 1. Tbx3 Is Dispensable in a Subpopulation of mESCs

(A) Picked long-term cultured Tbx3R mESC clones grown in presence (wDox) or absence (w/oDox) of Dox in ESC media containing LIF. BF, GFP channel, and AP staining colony pictures are shown. Scale bars represent 200  $\mu$ m.

(B) The mRNA expression signature of three independent Tbx3R-Dox mESC clones cultured in ESC media containing LIF. Data shown are the average of three independent clones for Tbx3R+Dox mESC.

(C) TBX3 protein expression in Tbx3R mESC clones cultured in ESC media containing LIF. Quantification of protein levels is shown.

(D) OCT4, SOX2, and TBX3 protein expression was checked by immunofluorescence (IF). Scale bars represent 200  $\mu$ m.

assay (Pereira and Fisher, 2009). We tested the ability of Tbx3<sup>N/N</sup> mESCs to confer an ESC-like state on human B cells following cell fusion (Figure S2F). The starting B cells do not express human TBX3 mRNA as shown using human-specific primers (Figure S2G). Tbx3<sup>N/N</sup> mESCs robustly induce a human ESC gene expression signature (Figure S2H) onto human B cells. Tbx3 null mESCs therefore retain the ability to reprogram differentiated cells into an ESC-like state, a property of self-renewing mESCs.

To rule out the possibility of cell culture side effects, we derived Tbx3<sup>-/-</sup> mESCs from Tbx3<sup>-/-</sup> blastocysts by mating Tbx3<sup>+/-</sup> mice (Figure S3A; Table S5). We refer to these in vivo derived cells as T3Blast mESCs. T3Blast<sup>+/+</sup>, T3Blast<sup>+/-</sup>, and T3Blast<sup>N/N</sup> cells maintain ESC-like morphology and stain positive for AP activity (Figure S3B). The mRNA expression levels of a selected panel of mESC genes did not change significantly (>2-fold) between T3Blast<sup>+/+</sup>, T3Blast<sup>+/-</sup>, and T3Blast<sup>N/N</sup> cells with the excep-

tion of *Dppa3* (Figure S3C). To further characterize the function of Tbx3 in vivo, we assessed Tbx3<sup>+/+</sup>, Tbx3<sup>+/-</sup>, and Tbx3<sup>-/-</sup> blastocysts at stages E3.75 and E4.5. They had no apparent abnormality in size (Figures S3D and S3E) and cell number (Figure S3E; Table S5). The number of cells expressing GATA6 and NANOG proteins, markers for primitive endoderm (PrE) and epiblast, respectively, were also assessed in the blastocysts. No significant difference was found between Tbx3<sup>+/+</sup>, Tbx3<sup>+/-</sup>, and Tbx3<sup>-/-</sup> blastocysts at stages E3.75 and E4.5 (Figure S3F). In summary, our data suggest that Tbx3 null mESCs can be derived, and they maintain a stable self-renewing state and contribute to live chimeric embryos upon blastocyst injection.

### Tbx3 Null mESCs Maintain an ESC-like Gene Expression Signature

To understand how ESC-like properties are maintained in the absence of Tbx3, we analyzed genome-wide mRNA

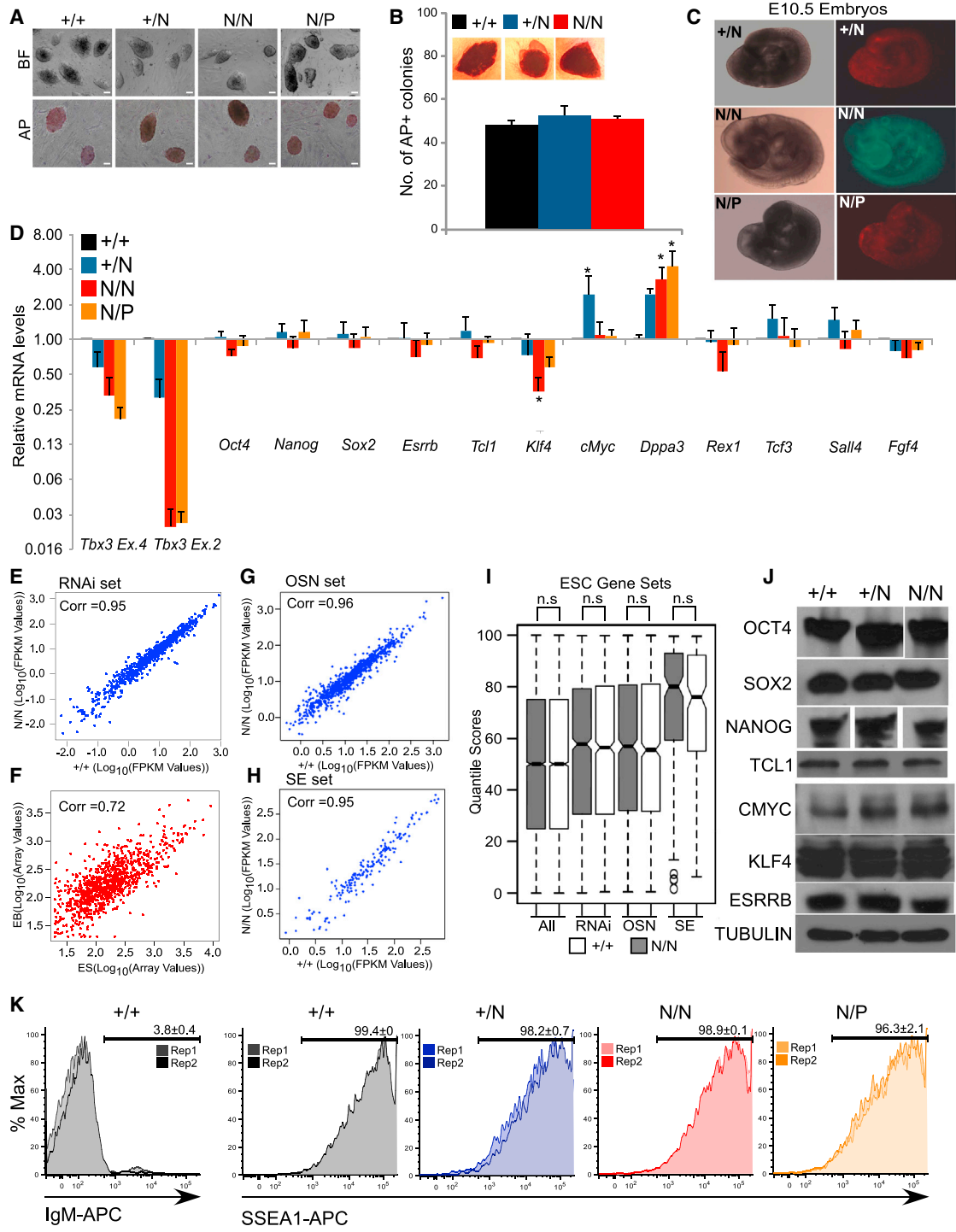


**Figure 2. Tbx3 Null mESCs Express an ESC-like Gene Expression Signature**

(A) Tbx3 null mESCs maintain ESC-like morphology (top) and AP activity (bottom). Scale bars represent 200  $\mu$ M.

(B) Single Tbx3 null mESCs sorted into 96-well plates and assayed for their ability to form AP-positive colonies. Data represent the average of two independent plates.

(C) Chimeric E10.5 embryos showing in vivo contribution of mESCs after blastocyst injection.

(D) mRNA levels of indicated ESC markers in mESCs cultured in the presence of LIF. Data are the average of three independent experiments.

\* $p < 0.05$  (t test).

(legend continued on next page)



expression profiles of  $Tbx3^{+/+}$ ,  $Tbx3^{+/N}$ , and  $Tbx3^{N/N}$  cells using mRNA-Seq (Table S1). Global gene expression profiles of  $Tbx3^{+/+}$ ,  $Tbx3^{+/N}$ , and  $Tbx3^{N/N}$  cells are strongly correlated with each other (0.96–0.98). We asked whether genes important for maintenance of the ESC state changed between  $Tbx3^{+/+}$ ,  $Tbx3^{+/N}$ , and  $Tbx3^{N/N}$  cells. To test this, we annotated a list of three ESC-specific gene sets. First, we looked at genes from published genome-wide RNAi screens in human and mouse ESCs that were found to be important for pluripotency, hereby-called “RNAi” set (Chia et al., 2010; Ding et al., 2009; Fazio et al., 2008; Hu et al., 2009; Kagey et al., 2010). Second, we analyzed genes whose upstream DNA elements are bound by Oct4, Sox2, and Nanog (OSN), hereby-called “OSN” set. Third, we looked at genes with transcriptional start sites (TSSs) closest to mESC-specific super enhancers, hereby called “SE” set (Chen et al., 2008; Marson et al., 2008b; Whyte et al., 2013). The genes from “RNAi” set are expressed at similar levels (correlation coefficient = 0.95) in  $Tbx3^{+/+}$  and  $Tbx3^{N/N}$  cells (Figure 2E). The mRNA expression pattern of the “RNAi” set genes between mESCs and mouse EBs (correlation coefficient = 0.72) is shown for comparison (Figure 2F) (Hailesellasse Sene et al., 2007). Also for genes from “OSN” and “SE” sets, mRNA expression levels correlated tightly (correlation coefficient = 0.95–0.96) between  $Tbx3^{+/+}$  and  $Tbx3^{N/N}$  cells (Figures 2G and 2H). We therefore, saw no significant changes in mRNA expression levels between  $Tbx3^{+/+}$  and  $Tbx3^{N/N}$  cells in any of the datasets tested (Figure 2I). In addition, we found comparable levels of key ESC proteins such as OCT4, SOX2, NANOG, ESRRB, CMYC, KLF4, and TCL1 in  $Tbx3^{+/+}$ ,  $Tbx3^{+/N}$ , and  $Tbx3^{N/N}$  cells (Figure 2J). The levels of SSEA1, a key cell surface marker of mESCs, also did not change between  $Tbx3^{+/+}$ ,  $Tbx3^{+/N}$ ,  $Tbx3^{N/N}$ , and  $Tbx3^{N/P}$  cells (Figure 2K). In conclusion,  $Tbx3$  null mESCs maintain a functionally unchanged global transcriptional landscape in long-term cultures.

### Tbx3 Transcriptionally Represses Dppa3 in mESCs

Our mRNA-Seq analysis revealed no global change in gene expression between  $Tbx3^{+/+}$ ,  $Tbx3^{+/N}$ , and  $Tbx3^{N/N}$  cells. However, few genes were upregulated (>2-fold) in  $Tbx3^{N/N}$  cells. *Dppa3* is one of those genes (Figure 2D). It is also upregulated in T3Blast<sup>N/N</sup> cells (Figure S3C). To investigate the

molecular mechanism of *Dppa3* induction, we expressed a Dox-inducible *Tbx3* transgene (Figure 3A) into  $Tbx3^{N/N}$  cells, hereby called  $Tbx3^{N/N}+Tg$  cells. Dox-induced *Tbx3* expression was verified at the mRNA and protein level (Figures S4A and S4B). *Tbx3* controls *Dppa3* mRNA expression in a concentration-dependent manner (Figure 3B). To confirm these results, we expressed Flag-Biotin-tagged *Tbx3* (fb*Tbx3*) transgene in  $Tbx3^{N/N}$  cells expressing the biotin ligase BirA transgene ( $Tbx3^{N/N}+BirA$  cells) (Figures 3C and 3D). The expression of the biotin ligase BirA allows for in vivo biotinylation of the tagged TBX3 protein (de Boer et al., 2003; Kim et al., 2009; Wang et al., 2006). Expression of fbTBX3 protein in  $Tbx3^{N/N}+BirA$  cells downregulated *Dppa3* mRNA expression (Figure 3E), while expression of other ESC TFs (*Nanog*, *Oct4*, *Rex1*) was unchanged. The effect of *Tbx3* expression on DPPA3 levels was also validated at the protein level using the cell lines discussed above (Figure 3F). *Dppa3* was also upregulated early upon shRNA-mediated depletion of *Tbx3* (*Tbx3R-Dox*) in a population of differentiating mESCs and in stable *Tbx3* knockdown clones (clones 15, 16, 17; discussed in Figure 1) (Figure 3G). We next asked whether *Tbx3* directly regulates the expression of *Dppa3* using ChIP-Seq in mESCs. TBX3 protein binds ~1.7 kb upstream of the *Dppa3* TSS (Figure 3H; Table S2). We also tested the expression of *Tbx3* and *Dppa3* mRNAs in 45 single mESCs. We confirmed that both *Tbx3* and *Dppa3* are heterogeneously expressed in a population of self-renewing (SSEA1+) mESCs (Figure 3I; Table S3), and their expression was anti-correlated ( $r = -0.61$ ,  $p = 0.05$ ) in cells that expressed *Tbx3* and *Dppa3* (Figure 3J). This anti-correlation of *Tbx3* and *Dppa3* expression in mESCs was also observed in other studies ( $r = -0.13$ ;  $p = 0.03$  in 185 cells) (Kumar et al., 2014). *Tbx3* therefore transcriptionally represses *Dppa3* in mESCs and may contribute to the heterogeneity of *Dppa3* expression.

*Dppa3* is a marker of naive mESCs downregulated in epiblast stem cells (EpiSCs) (Hayashi et al., 2008; Tesar et al., 2007) and during EB differentiation (Figure S4C). We therefore asked whether *Dppa3* overexpression compensates for absence of *Tbx3* and helps to maintain the mESC state. We utilized our genetic complementation strategy (Lee et al., 2012b) and established  $Tbx3^{N/N}$  cells stably expressing an shRNA targeting *Dppa3* as

(E–H) Correlation of mESC-specific gene set between WT and  $Tbx3^{N/N}$  cells. Genes that have effects on mESC self-renewal from published genome-wide RNAi screens (E). Correlation of the same gene set between ESCs and EBs (G). Genes whose promoters are bound by OCT4, SOX2, and NANOG (OSN) in mESCs from published datasets (F). Genes whose upstream or downstream DNA elements were described as ESC-specific super enhancers (H). “Corr” is the Pearson’s correlation coefficient.

(I) mRNA expression profile from normalized mRNA-Seq dataset from  $Tbx3^{+/+}$  and  $Tbx3^{N/N}$  mESCs for the indicated gene sets. The expression data are represented as quantile scores, described in Supplemental Information. Significance calculated using Wilcoxon rank sum test with continuity correction.

(J) Protein levels of indicated ESC markers in mESCs cultured in presence of LIF.

(K) SSEA1-APC staining on mESCs grown in serum + LIF. IgM-APC stained cells used as negative control.

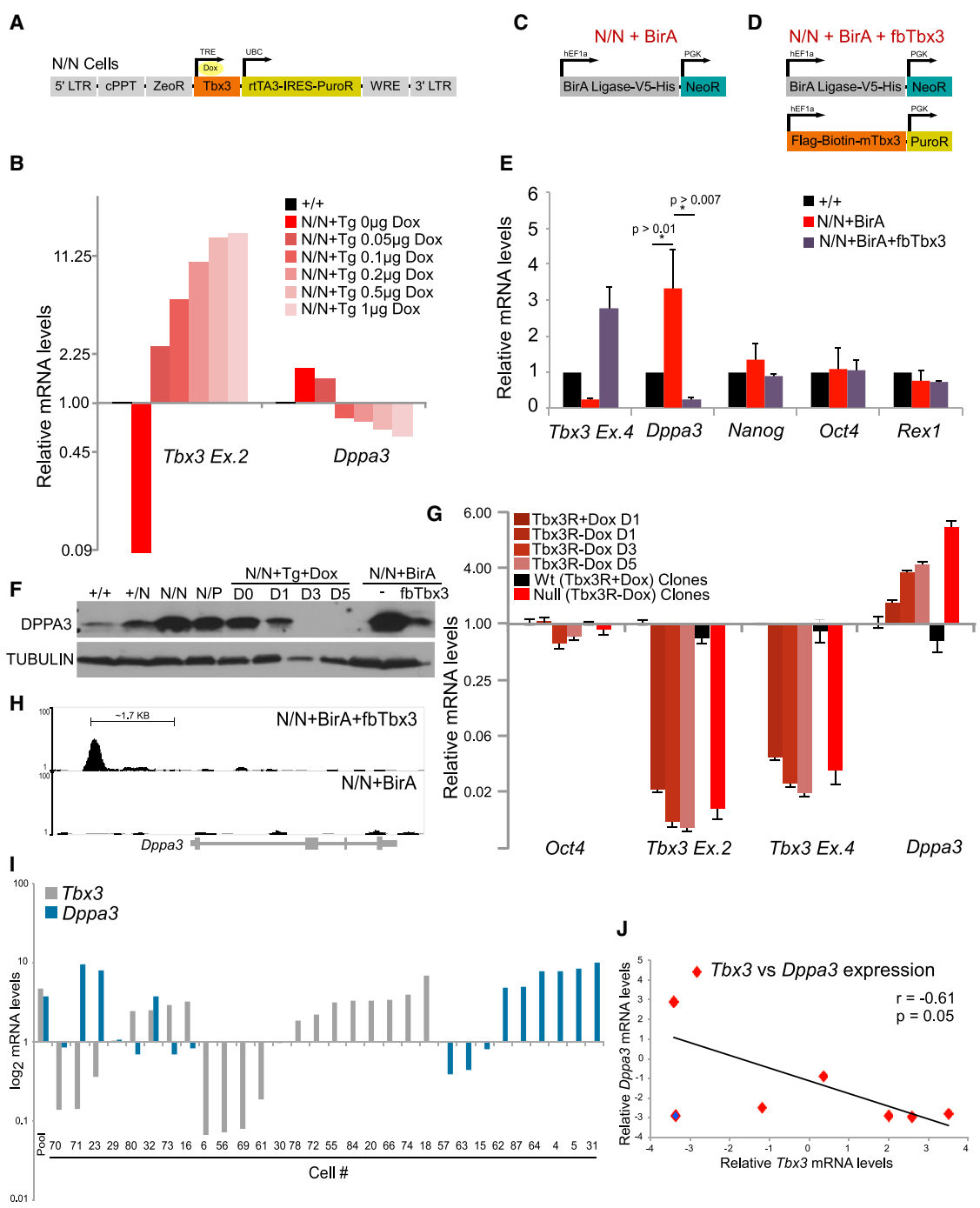


**Figure 3. Tbx3 Represses the Expression of Dppa3 in mESCs**

(A) Construct used for inducible expression of Tbx3 transgene in Tbx3 null mESCs.  
 (B) *Tbx3* and *Dppa3* mRNA levels in Tbx3<sup>+/+</sup> and Tbx3<sup>N/N</sup>+Tg cells treated with indicated concentrations of Dox/ml.  
 (C and D) Constructs used in making Tbx3<sup>N/N</sup> + BirA (C) and Tbx3<sup>N/N</sup> + BirA + fbTbx3 (D) lines.  
 (E) mRNA levels of indicated genes in Tbx3<sup>+/+</sup>, Tbx3<sup>N/N</sup>+BirA, and Tbx3<sup>N/N</sup>+BirA+fbTbx3 cells. Data are the average of three independent replicates. The p values were generated using t test.  
 (F) DPPA3 protein expression in Tbx3<sup>+/+</sup>, Tbx3<sup>N/N</sup>, Tbx3<sup>N/P</sup>, Tbx3<sup>N/N</sup>+Tg, Tbx3<sup>N/N</sup>+BirA, and Tbx3<sup>N/N</sup>+BirA+fbTbx3 cells.

(legend continued on next page)



well as a Dox-inducible shRNA immune Dppa3 Tg, named Tbx3<sup>N/N</sup>-Dp3R (Figure S4D). These rescue clones were generated in the presence of Dox (Figure S4E). Upon removal of Dox, Tbx3<sup>N/N</sup>-Dp3R cells displayed a partially differentiated morphology (Figure S4F) and decreased levels of the ESC marker SSEA1 (Figure S4G). These changes were accompanied by increased expression of the mesoderm marker Brachyury (*T*) and decreased expression of the ESC markers *Tcl1* and *Esrrb* (Figure S4H). Given this partial differentiation phenotype, it is likely that other factors besides Dppa3 also aid in the maintenance of the mESC state in the absence of Tbx3. Taken together, our results indicate that Dppa3 overexpression in Tbx3 null mESCs, at least in part, compensates for the function of Tbx3 in the maintenance of ESC state.

### Tbx3 Controls Initiation of Wnt Signaling-Mediated Mesoderm Differentiation

We wanted to better understand the function of Tbx3 during the exit of mESCs from pluripotency toward differentiation. During exit from pluripotency, *Tbx3* expression is downregulated (Figure S4I). *Tbx3* expression is also downregulated in mouse EpiSCs (Tesar et al., 2007) and mouse epiblast-like stem cells (EpiLCs) (Buecker et al., 2014). We used Wnt mediated serum-free derivation of mesoderm from mESCs to further assess levels of *Tbx3* (Figure S4J) (Kanke et al., 2014). During 2 days of differentiation, mesoderm genes (*T*, *Mixl1*, *Wnt8a*) were upregulated (Figure S4K), and other pluripotency-associated genes (*Nanog*, *Tcl1*) as well as *Tbx3* were downregulated (Figure S4L).

We tested the ability of Tbx3 null mESCs to differentiate into the three germ layers using the EB differentiation assay. Absence of *Tbx3* expression in Tbx3<sup>N/N</sup> cells is accompanied by overexpression of *Dppa3* (Figure 4A), a number of markers of ectoderm (*Mash1/Ascl1*, *Nes*) (Figure 4B), mesoderm (*T*, *Mixl1*, *Flk1*, *Tbx6*) (Figure 4C), and mesoderm (*Cxcr4*) markers (Figure 4D). However, endoderm (*Gata6*, *Sox17*, *Foxa2*) and extraembryonic endoderm (*Sox7*, *Amn*) genes were significantly downregulated in EBs of Tbx3<sup>N/N</sup> cells (Figures 4E and 4F), consistent with the reported role of Tbx3 in regulating extraembryonic endoderm differentiation (Kartikasari et al., 2013; Lu et al., 2011). We confirmed these results by knocking down Tbx3 in mESCs using shRNA and testing its effect on EB differentiation (Figure 4G). *Tbx3* expression was downregulated, and *Dppa3* expression was significantly upregulated

(Figure 4H). We saw significant upregulation of mesoderm (*T*, *Flk1*, *Mixl1*) and ectoderm (*Nes*) genes (Figures 4I and 4J), while endoderm gene (*Sox17*) was downregulated (Figure 4K). The same effect was also seen during differentiation of Tbx3<sup>N/P</sup> cells. In absence of *Tbx3* expression (Figure S5A), *Dppa3* was upregulated (Figure S5B). The upregulation of mesoderm genes (*T*, *Tbx6*, *Wnt8a*) (Figure S5C) and downregulation of endoderm genes (*Sox17*, *FoxA2*, *Gata6*, *Amn*, *Sox7*) (Figure S5D) were confirmed. To confirm the effect at the protein level, we used a serum-free differentiation (SFD) protocol to direct mESCs to mesoderm progenitors (Figure S5E). Mesoderm progenitors are ECADHERIN<sup>-</sup> FLK1<sup>+</sup> population (Nostro et al., 2008; Yamashita et al., 2000; Yasunaga et al., 2005). A population of ECADHERIN<sup>-</sup> mesoderm cells also expresses CXCR4 protein unlike endoderm cells that are ECADHERIN<sup>+</sup> CXCR4<sup>+</sup> (Yasunaga et al., 2005). Therefore, to define mesoderm progenitors, we measured either ECADHERIN<sup>-</sup> FLK1<sup>+</sup> or ECADHERIN<sup>-</sup> FLK1<sup>+</sup> CXCR4<sup>+</sup> after 5–6 days of differentiation of Tbx3<sup>+/+</sup>, Tbx3<sup>+/N</sup>, and Tbx3<sup>N/P</sup> cells (Figure S5F). We see a significant upregulation of mesoderm differentiation in Tbx3<sup>N/P</sup> cells compared with Tbx3<sup>+/+</sup> cells (Figure S5G). Tbx3 therefore represses differentiation into mesoderm lineage.

Furthermore, in ESC growth conditions, knockdown of Tbx3 in mESCs (shTbx3) causes a significant upregulation of mesoderm genes (Figure 5A). *T*, a primitive streak marker, is overexpressed in shTbx3 cells (~60-fold) (Figure 5B). Wnt signaling regulates and is regulated by *T* expression during primitive streak emergence and early mesoderm formation (Martin and Kimelman, 2010; Narayanan et al., 2011; Yamaguchi et al., 1999). We saw that shTbx3 cells have significantly increased expression of Wnt pathway genes (Figures S6A). Specifically, *Wnt8a* and *Fzd2* mRNAs are upregulated in shTbx3 cells (Figures 5C and 5D). *Wnt8a* is expressed during early stages of mESC differentiation (Lindsley et al., 2006) and in mesoderm progenitors of a developing embryo (Narayanan et al., 2011). During a time course of EB differentiation, *Wnt8a* and *Fzd2* are significantly upregulated in EBs derived from Tbx3 null cells (Figure 5E) and in EBs derived upon knockdown of Tbx3 (Figure 5F). TBX3 protein also binds upstream of the *T*, *Wnt8a*, and *Fzd2* gene promoters in mESCs (Figures 5G–5I; Table S2) directly repressing their expression.

Apart from its role in differentiation, Wnt signaling is known to promote pluripotency in ESC culture conditions.

(G) mRNA expression profile from qRT-PCR experiment for the indicated genes. Tbx3R data are cells grown with or without Dox (Tbx3) over 5 days. Wild-type (Tbx3R+Dox) data are an average of three independent clones 27, 28, and 29 from Figure 1. Null (Tbx3R-Dox) data are an average of three independent clones 15, 16, and 17 from Figure 1.

(H) TBX3 binds 1.7 kb upstream of the *Dppa3* TSS in mESCs.

(I) *Tbx3* and *Dppa3* mRNA levels in SSEA1<sup>+</sup> single mESCs.

(J) Correlation of mRNA expression values in cells expressing *Dppa3* and *Tbx3*.

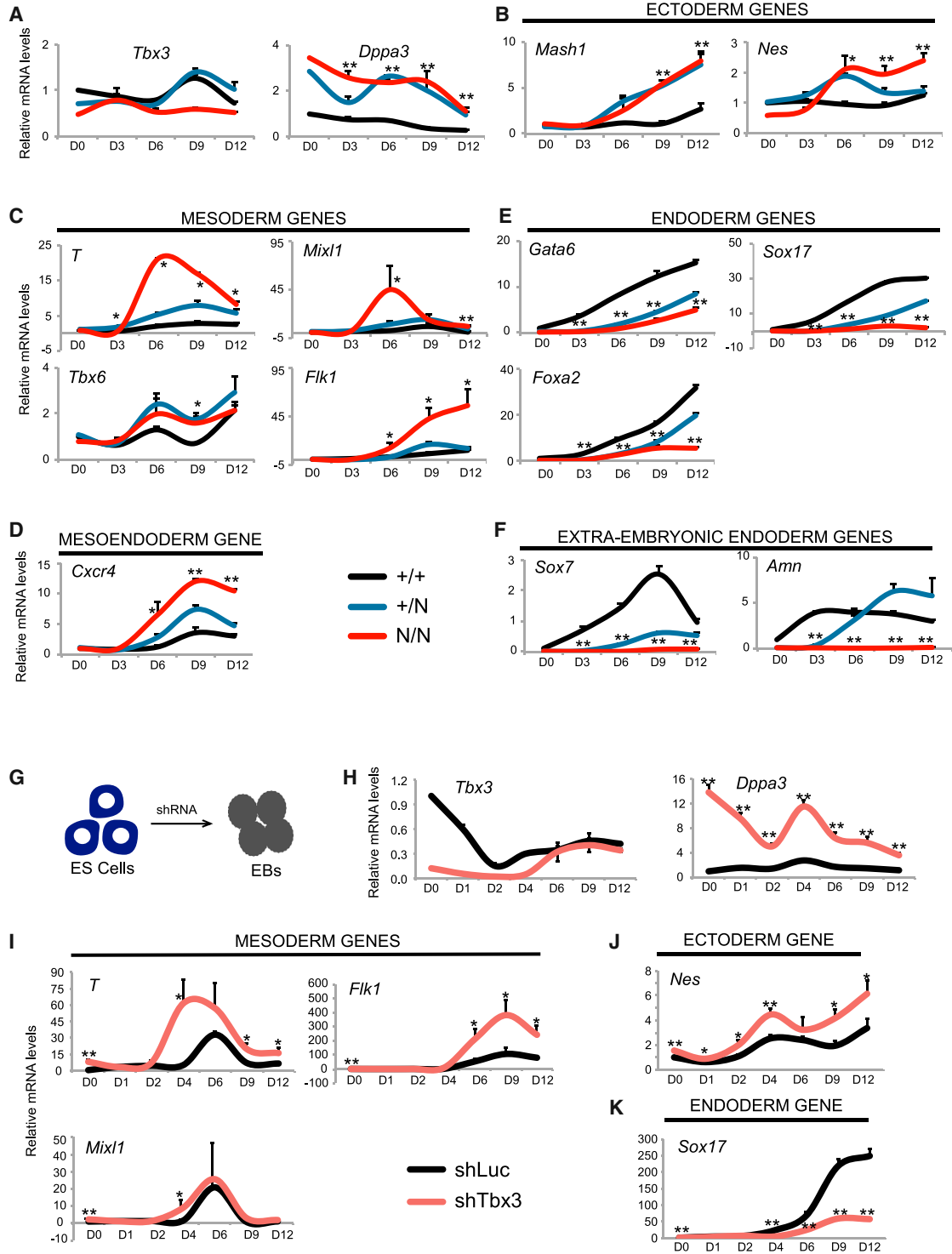


**Figure 4. Effect of Tbx3's Loss on Differentiation of mESCs**

(A–F) The mRNA expression pattern of indicated genes during a 12-day EB differentiation time course. Data are average of three independent replicates. \* $p < 0.05$  and \*\* $p < 0.005$  (t test).

(G) Schematic of EB differentiation of mESCs after infection with the control shRNA or Tbx3 shRNA.

(H–K) The mRNA expression pattern of indicated genes during a 12-day EB differentiation time course after infection with the control shRNA or Tbx3 shRNA. The data are an average of three independent replicates. \* $p < 0.05$  and \*\* $p < 0.005$  (t test).

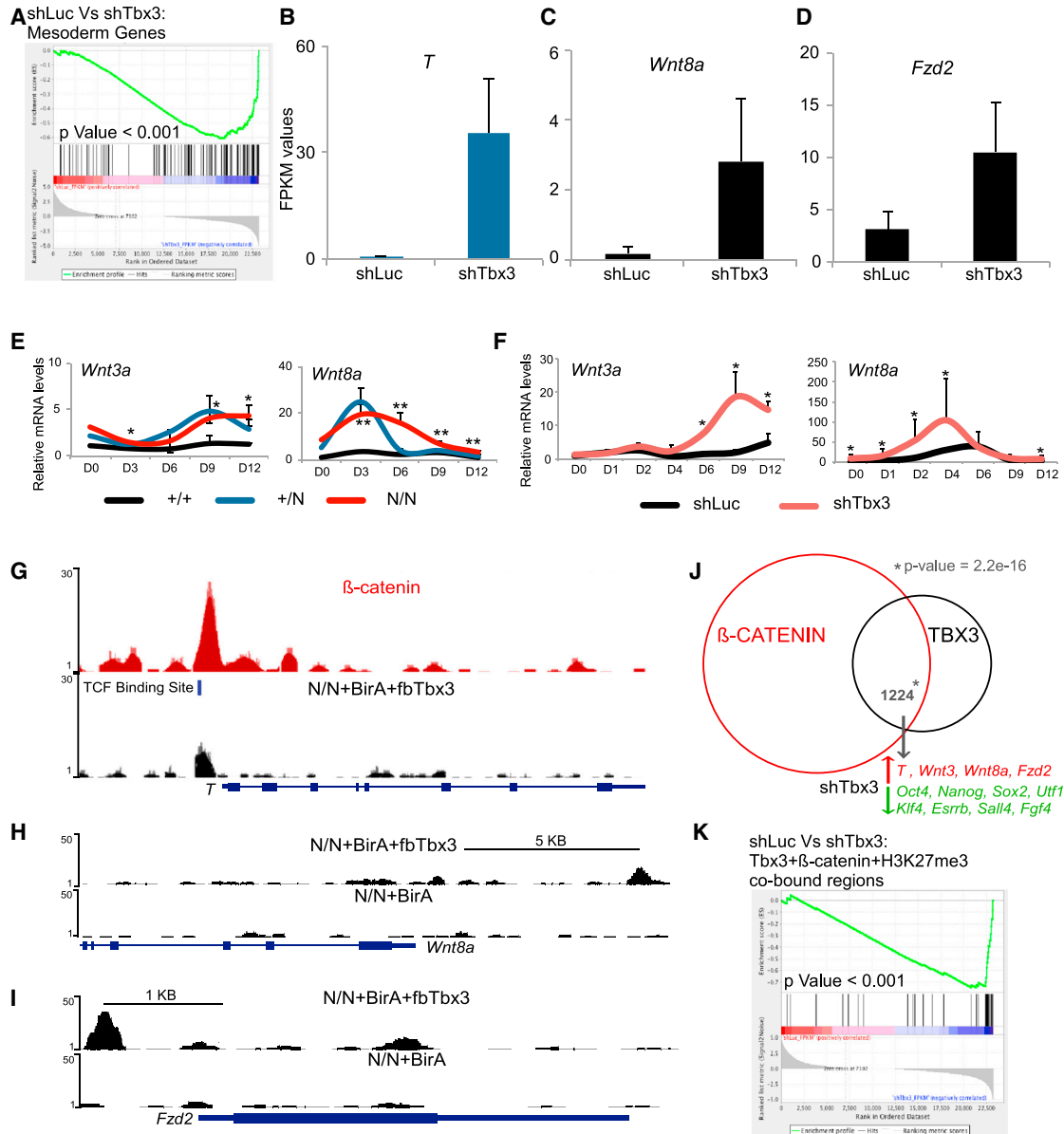


**Figure 5. Tbx3 Represses Wnt Signaling-Mediated Mesoderm Differentiation**

(A) Gene set enrichment analysis (GSEA) to detect statistical significance of mesoderm genes in shTbx3 versus shLuc. Cells grown in ESC media containing LIF were infected with lentiviral shRNA constructs against Luciferase (shLuc) or Tbx3 (shTbx3).

(B–D) mRNA-Seq FPKM values of *T*, *Wnt8a*, and *Fzd2* in cells infected the indicated shRNAs.

(E) mRNA expression profile of indicated genes during EB differentiation time course of 12 days for indicated cell lines. Data are the average of three independent replicates. \* $p < 0.05$  and \*\* $p < 0.005$  (t test).

(F) mRNA expression profile of the indicated genes during EB differentiation time course of 12 days in WT mESCs infected with indicated shRNAs. Data are the average of three independent replicates. \* $p < 0.05$  and \*\* $p < 0.005$  (t test).

(G–I) TBX3 ChIP-seq binding data from N/N-BirA (control) and N/N-BirA+fbTbx3 cells.  $\beta$ -CATENIN binding from published data.

(J) Venn diagram representing overlap between  $\beta$ -CATENIN and TBX3 genome-wide binding sites. The p value was generated using the fisher exact test.

(K) GSEA to detect statistical significance of TBX3,  $\beta$ -CATENIN, and H3K27me3 co-bound gene set in shTbx3 versus shLuc.

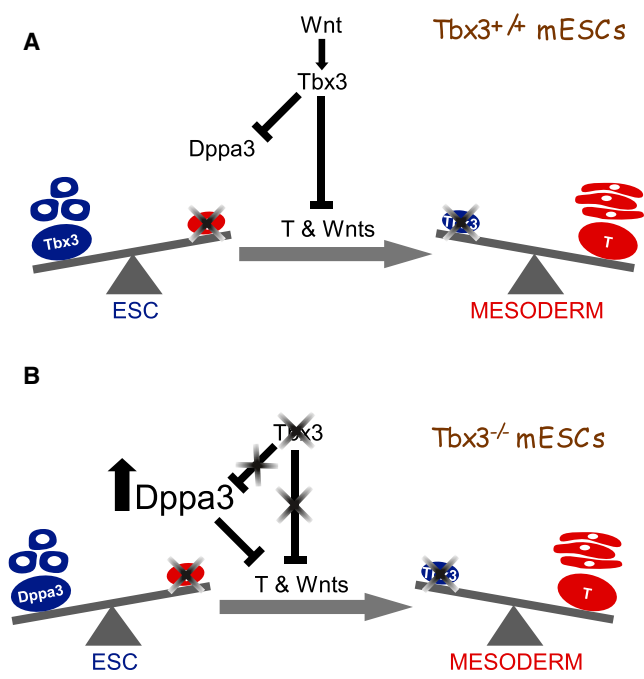


**Figure 6. Tbx3-Mediated Repression of *Dppa3*, Mesoderm Genes, and Wnt Signaling Components Maintains the Balance between Self-renewal and Differentiation of mESCs**

(A) In WT mESCs, *Tbx3* controls expression of *Dppa3*, mesoderm genes, and Wnt signaling components to maintain mESC pluripotency.

(B) In *Tbx3* null mESCs, *Dppa3* is overexpressed and partially takes over function of *Tbx3* to repress mesoderm genes and Wnt signaling components to maintain mESC pluripotency.

The addition of WNT3A into mESC culture media increased levels of *Tbx3* mRNA (Figures S5B and S5C). A significant number of genes bound by TBX3 are also bound by  $\beta$ -CATENIN, a downstream effector of Wnt signaling (Figure 5J). We found that the TBX3 binding site upstream of the *T* promoter (Figure 5G) overlaps with a TCF binding motif previously shown to activate *T* expression during mesoderm differentiation (Yamaguchi et al., 1999). This binding site is also co-bound by  $\beta$ -CATENIN upon Wnt stimulation (Figure 5G) in mESCs (Zhang et al., 2013) and mediates the differentiation of human ESCs and iPSCs into mesoderm lineage (Mendjan et al., 2014). This region is also marked by repressive modification H3K27me3 in mESCs (encode data). A significant number of TBX3 and  $\beta$ -CATENIN co-bound genes are highly expressed in mESCs, including *Oct4*, *Nanog*, *Sox2*, and *Esrrb* (Figure S5D). However, TBX3,  $\beta$ -CATENIN, and H3K27me3 co-bound genes are significantly upregulated upon knockdown of *Tbx3*, which included mesoderm genes such as *T*, *Wnt8a*, *Hes7* (Figure 5K). Therefore, *Tbx3* along with  $\beta$ -catenin represses mesoderm and Wnt pathway genes required for initiation of mesoderm differentiation.

*Tbx3* is rapidly downregulated upon differentiation of mESCs and is subsequently upregulated during later stages of differentiation. To address the role of *Tbx3* during the exit from pluripotency, we overexpressed *Tbx3* in WT mESCs prior to and during differentiation (Figure S6E). Overexpression of *Tbx3* for 2 days prior to differentiation repressed expression of mesoderm genes (*T*, *Mixl1*, *Tbx6*) and Wnt genes required for mesoderm differentiation (*Wnt8a*, *Wnt3a*) (Figure S6F). Collectively, these data indicate that *Tbx3* plays two separate roles, one during exit from pluripotency where it represses mesoderm genes and another during gastrulation, as reported, where it promotes the development of a mesendoderm population (Weidgang et al., 2013). In pluripotent *Tbx3* null cells, but not in WT cells (data not shown), *Dppa3* is overexpressed and represses *T* and *Wnt8a* (Figure S6G). *Dppa3* therefore compensates for *Tbx3* function in repressing mesoderm differentiation and maintains pluripotency in the absence of *Tbx3*. Taken together, these findings suggest *Tbx3* orchestrates the exit of mESCs from pluripotency by directly regulating members of the Wnt signaling pathway and repressing expression of mesoderm genes (Figures 6A and 6B).

## DISCUSSION

Many key pluripotency TFs bind within close proximity to specific genomic locations and therefore cooperatively control the expression of key genes (Chen et al., 2008). Overlapping functional TF binding sites (Whyte et al., 2013) ensure the stability of the overall transcriptional network. At the same time, TF expression heterogeneity (Chambers et al., 2007; Kumar et al., 2014; MacArthur and Lemischka, 2013; MacArthur et al., 2012; Niwa et al., 2009; Toyooka et al., 2008) allows the network to respond quickly and specifically to external differentiation cues. We expect there exists *Tbx3* high and low self-renewing states in an ESC population. Such states maybe dynamic and possess different developmental potentials. In the absence of *Tbx3*, mESCs can self-renew in LIF containing media and maintain an alternate and stable pluripotent state. Like other ESC TFs such as *Nanog* and *Sox2* (Thomson et al., 2011), *Tbx3* maintains the pluripotent state and promotes differentiation into specific lineages like embryonic and extra-embryonic endoderm (Kartikasari et al., 2013; Lu et al., 2011).

Using a loss-of-function approach, we identify direct versus indirect targets of *Tbx3* in mESCs. *Tbx3* maintains normal steady-state levels of *Dppa3*. In the absence of *Tbx3*, upregulation of *Dppa3* in part contributes to the maintenance of a stable pluripotent state. Varying levels of *Dppa3* in mESCs marks distinct developmental states



(Hayashi et al., 2008). The mechanisms by which expression heterogeneity of *Dppa3* is maintained in mESCs have not been defined. *Tbx3* prevents the overexpression of *Dppa3* in mESCs and may contribute to its heterogeneous expression.

Downstream components of key signaling pathways such as Bmp/Smad, Lif/Stat (Niwa et al., 1998; van Oosten et al., 2012), Wnt/ $\beta$ -catenin (Habib et al., 2013; Merrill, 2012), and PI3K/Akt (Niwa et al., 2009) balance self-renewal and differentiation. External signaling cues integrate into a response generated by activation or repression of key lineage-specific TFs (Chen et al., 2008; Lee et al., 2012a; Mullen et al., 2011; Niwa et al., 2009). *Tbx3* expression is regulated by key signaling cascades such as Bmp/Smad (Chen et al., 2008; Yang et al., 2006), Jak/Stat (Chen et al., 2008), PI3K/Akt (Niwa et al., 2009), Grb2/Mapk (Niwa et al., 2009), and Wnt/ $\beta$ -catenin (Price et al., 2013; Renard et al., 2007). Wnt signaling and Mapk inhibition in particular play important roles in pluripotency (ten Berge et al., 2011) and mesoderm differentiation (Gadue et al., 2006). Activation of Wnt signaling by repression of GSK3 $\beta$  alone stimulates mesoderm differentiation from mESCs grown in ground state condition (Kanke et al., 2014; Ying et al., 2008). In vivo loss-of-function studies demonstrate the requirement of Wnt signaling in the generation of primitive streak during gastrulation (Tortelote et al., 2013; Yamaguchi et al., 1999). Wnt signaling is transduced by regulation of TFs such as Tcf1 and Tcf3 (Yi et al., 2011; Zhang et al., 2013). We show that downstream of Wnt signaling *Tbx3* is required to repress premature differentiation of mESCs into mesoderm cells. We propose that the seemingly paradoxical functions of the Wnt signaling pathway in pluripotency versus differentiation are mediated in part through its control of *Tbx3* expression. In the absence of *Tbx3* expression, overexpression of *T* and Wnt pathway genes such as *Wnt8a* promotes mesoderm differentiation. *Tbx3* therefore fine tunes the response of Wnt signaling to maintain the balance between pluripotency and mesoderm differentiation.

Recent studies indicated that overexpression of *Tbx3* in differentiating cell populations promotes differentiation toward a mesendoderm fate (Kartikasari et al., 2013; Weidgang et al., 2013). We show that overexpression of *Tbx3* in mESCs prior to differentiation blocks emergence of mesoderm lineage (Ivanova et al., 2006; Lu et al., 2011). *Tbx3* expression is downregulated during the early stages of differentiation and upregulated at later stages (Hailesellasse Sene et al., 2007; Hayashi et al., 2008). *Tbx3* expression is also highly downregulated during in vivo development of epiblast from the ICM and in the in vitro established EpiSCs and EpiLCs (Brons et al., 2007; Buecker et al., 2014; Tesar et al., 2007). *Tbx3* therefore has a dual role in blocking the premature exit from pluripotency by directly

repressing mesoderm and Wnt pathway genes and at a later stage by promoting mesoderm differentiation during gastrulation.

Collectively, we suggest a model in which interplay of *Tbx3* and *Dppa3* regulates early differentiation decisions into mesoderm lineage by controlling components of Wnt pathway and mesoderm genes in response to external cues. The regulation of *Dppa3* expression by *Tbx3* in mESCs may act as a “buffer” to allow responses to varying concentrations of these two key TFs, thus maintaining a dynamic and responsive transcriptional landscape. Our model reconciles the dual role of Wnt signaling in maintaining the balance between mESC self-renewal versus differentiation. In conclusion, since *Tbx3* is downstream of key signaling cascades and overlaps with many TF circuits understanding the direct versus indirect targets of *Tbx3* and mechanisms by which it maintains pluripotency is vital to understanding the process of differentiation from self-renewing mESCs.

## EXPERIMENTAL PROCEDURES

### Cell Culture

The mESCs in the study were generated from R1, J1, AINV15, KH2, and CCE mESC lines. *Tbx3* null mESCs were generated from *Tbx3*<sup>+/-</sup> cells (Davenport et al., 2003). The procedures followed to make the lines are mentioned in greater detail in [Supplemental Information](#).

### Differentiation Assays in Serum and Serum-free Conditions

EB differentiation assay was performed in serum containing media without LIF by plating 0.5- to 2-million cells per well of a low attachment six-well plate over a time course of days. Serum-free mesoderm differentiation assay were performed as described (Gouon-Evans et al., 2006). Briefly, mESCs were plated in low attachment plates for 48 hr in SFD media and then replated in the same plates with VEGF (5 ng/ $\mu$ l), ACTIVIN A (25 ng/ $\mu$ l), and BMP4 (2.5 ng/ $\mu$ l). The cells were stained with respective antibodies (Table S4) and analyzed by FACS described in [Supplemental Information](#).

### ChIP-Seq and mRNA-Seq

ChIP-Seq experiment was done as described (Ang et al., 2011). mRNA-Seq experiment was done using the polyA pull down method as described in [Supplemental Information](#). Sequencing analysis for ChIP-seq and mRNA-seq data were performed in house as described in supplemental methods (Tables S1 and S2). Raw data were deposited in Gene Expression Omnibus (GEO), accession number GSE60066.

### Blastocyst Injection Assay

Indicated mESCs were injected into isolated C7Bl6 blastocysts and placed into pseudo-pregnant mice at the mouse genetics core at



Mount Sinai. The embryos were harvested at E10.5, and pictures were taken using a fluorescence microscope. Mouse work was subject to approval by and carried out in accordance with guidelines from Mount Sinai's Institutional Animal Care and Use Committee.

## SUPPLEMENTAL INFORMATION

Supplemental Information includes Supplemental Experimental Procedures, six figures, and six tables and can be found with this article online at <http://dx.doi.org/10.1016/j.stemcr.2015.05.009>.

## ACKNOWLEDGMENTS

We thank Dr. E. Bernstein, Dr. M. Rendl, Dr. J. Wang and Dr. P. Soriano, Dr. V. Gouon-Evans, and their laboratories for their critical guidance and assistance. We thank members of the Lemischka/Moore laboratory for useful discussions. This research was funded by grants from the NIH (5R01GM078465) to I.R.L. B.C. is a trainee in NIDCR-Interdisciplinary Training in Systems and Developmental Biology and Birth Defects (T32HD075735). A.G.F. was supported by Fundação para a Ciência e a Tecnologia-FCT (SFRH/BD/64715/2009).

Received: August 7, 2014

Revised: May 14, 2015

Accepted: May 18, 2015

Published: June 18, 2015

## REFERENCES

Ang, Y.S., Tsai, S.Y., Lee, D.F., Monk, J., Su, J., Ratnakumar, K., Ding, J., Ge, Y., Darr, H., Chang, B., et al. (2011). *Wdr5* mediates self-renewal and reprogramming via the embryonic stem cell core transcriptional network. *Cell* *145*, 183–197.

Arnold, S.J., Stappert, J., Bauer, A., Kispert, A., Herrmann, B.G., and Kemler, R. (2000). *Brachyury* is a target gene of the *Wnt*/ $\beta$ -catenin signaling pathway. *Mech. Dev.* *91*, 249–258.

Brons, I.G., Smithers, L.E., Trotter, M.W., Rugg-Gunn, P., Sun, B., Chuvpova, S.M., Howlett, S.K., Clarkson, A., Ahrlund-Richter, L., Pedersen, R.A., and Vallier, L. (2007). Derivation of pluripotent epiblast stem cells from mammalian embryos. *Nature* *448*, 191–195.

Buecker, C., Srinivasan, R., Wu, Z., Calo, E., Acampora, D., Faial, T., Simeone, A., Tan, M., Swigut, T., and Wysocka, J. (2014). Reorganization of enhancer patterns in transition from naive to primed pluripotency. *Cell Stem Cell* *14*, 838–853.

Chambers, I., Silva, J., Colby, D., Nichols, J., Nijmeijer, B., Robertson, M., Vrana, J., Jones, K., Grotewold, L., and Smith, A. (2007). *Nanog* safeguards pluripotency and mediates germline development. *Nature* *450*, 1230–1234.

Chapman, D.L., Garvey, N., Hancock, S., Alexiou, M., Agulnik, S.I., Gibson-Brown, J.J., Cebra-Thomas, J., Bollag, R.J., Silver, L.M., and Papaioannou, V.E. (1996). Expression of the T-box family genes, *Tbx1*–*Tbx5*, during early mouse development. *Dev. Dyn.* *206*, 379–390.

Chen, X., Xu, H., Yuan, P., Fang, F., Huss, M., Vega, V.B., Wong, E., Orlov, Y.L., Zhang, W., Jiang, J., et al. (2008). Integration of external

signaling pathways with the core transcriptional network in embryonic stem cells. *Cell* *133*, 1106–1117.

Chia, N.Y., Chan, Y.S., Feng, B., Lu, X., Orlov, Y.L., Moreau, D., Kumar, P., Yang, L., Jiang, J., Lau, M.S., et al. (2010). A genome-wide RNAi screen reveals determinants of human embryonic stem cell identity. *Nature* *468*, 316–320.

Davenport, T.G., Jerome-Majewska, L.A., and Papaioannou, V.E. (2003). Mammary gland, limb and yolk sac defects in mice lacking *Tbx3*, the gene mutated in human ulnar mammary syndrome. *Development* *130*, 2263–2273.

de Boer, E., Rodriguez, P., Bonte, E., Krijgsvelde, J., Katsantoni, E., Heck, A., Grosveld, F., and Strouboulis, J. (2003). Efficient biotinylation and single-step purification of tagged transcription factors in mammalian cells and transgenic mice. *Proc. Natl. Acad. Sci. USA* *100*, 7480–7485.

Ding, L., Paszkowski-Rogacz, M., Nitzsche, A., Slabicki, M.M., Heninger, A.-K., de Vries, I., Kittler, R., Junqueira, M., Shevchenko, A., Schulz, H., et al. (2009). A genome-scale RNAi screen for *Oct4* modulators defines a role of the *Paf1* complex for embryonic stem cell identity. *Cell Stem Cell* *4*, 403–415.

Evans, M.J., and Kaufman, M.H. (1981). Establishment in culture of pluripotential cells from mouse embryos. *Nature* *292*, 154–156.

Faddah, D.A., Wang, H., Cheng, A.W., Katz, Y., Buganim, Y., and Jaenisch, R. (2013). Single-cell analysis reveals that expression of *nanog* is biallelic and equally variable as that of other pluripotency factors in mouse ESCs. *Cell Stem Cell* *13*, 23–29.

Fazio, T.G., Huff, J.T., and Panning, B. (2008). An RNAi screen of chromatin proteins identifies *Tip60*–*p400* as a regulator of embryonic stem cell identity. *Cell* *134*, 162–174.

Gadue, P., Huber, T.L., Paddison, P.J., and Keller, G.M. (2006). *Wnt* and *TGF- $\beta$*  signaling are required for the induction of an in vitro model of primitive streak formation using embryonic stem cells. *Proc. Natl. Acad. Sci. USA* *103*, 16806–16811.

Gouon-Evans, V., Boussemaert, L., Gadue, P., Nierhoff, D., Koehler, C.I., Kubo, A., Shafritz, D.A., and Keller, G. (2006). *BMP-4* is required for hepatic specification of mouse embryonic stem cell-derived definitive endoderm. *Nat. Biotechnol.* *24*, 1402–1411.

Habib, S.J., Chen, B.C., Tsai, F.C., Anastasiadis, K., Meyer, T., Betzig, E., and Nusse, R. (2013). A localized *Wnt* signal orients asymmetric stem cell division in vitro. *Science* *339*, 1445–1448.

Hailesellasse Sene, K., Porter, C.J., Palidwor, G., Perez-Iratxeta, C., Muro, E.M., Campbell, P.A., Rudnicki, M.A., and Andrade-Navarro, M.A. (2007). Gene function in early mouse embryonic stem cell differentiation. *BMC Genomics* *8*, 85.

Han, J., Yuan, P., Yang, H., Zhang, J., Soh, B.S., Li, P., Lim, S.L., Cao, S., Tay, J., Orlov, Y.L., et al. (2010). *Tbx3* improves the germline competency of induced pluripotent stem cells. *Nature* *463*, 1096–1100.

Hayashi, K., Lopes, S.M., Tang, F., and Surani, M.A. (2008). Dynamic equilibrium and heterogeneity of mouse pluripotent stem cells with distinct functional and epigenetic states. *Cell Stem Cell* *3*, 391–401.

Ho, R., Papp, B., Hoffman, J.A., Merrill, B.J., and Plath, K. (2013). Stage-specific regulation of reprogramming to induced pluripotent



- stem cells by Wnt signaling and T cell factor proteins. *Cell Rep* 3, 2113–2126.
- Hu, G., Kim, J., Xu, Q., Leng, Y., Orkin, S.H., and Elledge, S.J. (2009). A genome-wide RNAi screen identifies a new transcriptional module required for self-renewal. *Genes Dev.* 23, 837–848.
- Ivanova, N., Dobrin, R., Lu, R., Kotenko, I., Levorse, J., DeCoste, C., Schafer, X., Lun, Y., and Lemischka, I.R. (2006). Dissecting self-renewal in stem cells with RNA interference. *Nature* 442, 533–538.
- Kagey, M.H., Newman, J.J., Bilodeau, S., Zhan, Y., Orlando, D.A., van Berkum, N.L., Ebmeier, C.C., Goossens, J., Rahl, P.B., Levine, S.S., et al. (2010). Mediator and cohesin connect gene expression and chromatin architecture. *Nature* 467, 430–435.
- Kanke, K., Masaki, H., Saito, T., Komiyama, Y., Hojo, H., Nakauchi, H., Lichtler, A.C., Takato, T., Chung, U.I., and Ohba, S. (2014). Stepwise differentiation of pluripotent stem cells into osteoblasts using four small molecules under serum-free and feeder-free conditions. *Stem Cell Rev.* 2, 751–760.
- Kartikasari, A.E., Zhou, J.X., Kanji, M.S., Chan, D.N., Sinha, A., Grapin-Botton, A., Magnuson, M.A., Lowry, W.E., and Bhushan, A. (2013). The histone demethylase Jmjd3 sequentially associates with the transcription factors Tbx3 and Eomes to drive endoderm differentiation. *EMBO J.* 32, 1393–1408.
- Kelly, K.F., Ng, D.Y., Jayakumar, G., Wood, G.A., Koide, H., and Doble, B.W. (2011).  $\beta$ -catenin enhances Oct-4 activity and reinforces pluripotency through a TCF-independent mechanism. *Cell Stem Cell* 8, 214–227.
- Kemp, C., Willems, E., Abdo, S., Lambiv, L., and Leyns, L. (2005). Expression of all Wnt genes and their secreted antagonists during mouse blastocyst and postimplantation development. *Dev. Dyn.* 233, 1064–1075.
- Kim, J., Cantor, A.B., Orkin, S.H., and Wang, J. (2009). Use of in vivo biotinylation to study protein-protein and protein-DNA interactions in mouse embryonic stem cells. *Nat. Protoc.* 4, 506–517.
- Kumar, R.M., Cahan, P., Shalek, A.K., Satija, R., DaleyKeyser, A.J., Li, H., Zhang, J., Pardee, K., Gennert, D., Trombetta, J.J., et al. (2014). Deconstructing transcriptional heterogeneity in pluripotent stem cells. *Nature* 516, 56–61.
- Lee, D.F., Su, J., Ang, Y.S., Carvajal-Vergara, X., Mulero-Navarro, S., Pereira, C.F., Gingold, J., Wang, H.L., Zhao, R., Sevilla, A., et al. (2012a). Regulation of embryonic and induced pluripotency by aurora kinase-p53 signaling. *Cell Stem Cell* 11, 179–194.
- Lee, D.F., Su, J., Sevilla, A., Gingold, J., Schaniel, C., and Lemischka, I.R. (2012b). Combining competition assays with genetic complementation strategies to dissect mouse embryonic stem cell self-renewal and pluripotency. *Nat. Protoc.* 7, 729–748.
- Liang, G., and Zhang, Y. (2013). Embryonic stem cell and induced pluripotent stem cell: an epigenetic perspective. *Cell Res.* 23, 49–69.
- Lim, C.Y., Tam, W.L., Zhang, J., Ang, H.S., Jia, H., Lipovich, L., Ng, H.H., Wei, C.L., Sung, W.K., Robson, P., et al. (2008). Sall4 regulates distinct transcription circuitries in different blastocyst-derived stem cell lineages. *Cell Stem Cell* 3, 543–554.
- Lindsley, R.C., Gill, J.G., Kyba, M., Murphy, T.L., and Murphy, K.M. (2006). Canonical Wnt signaling is required for development of embryonic stem cell-derived mesoderm. *Development* 133, 3787–3796.
- Loh, K.M., and Lim, B. (2011). A precarious balance: pluripotency factors as lineage specifiers. *Cell Stem Cell* 8, 363–369.
- Loh, Y.H., Zhang, W., Chen, X., George, J., and Ng, H.H. (2007). Jmjd1a and Jmjd2c histone H3 Lys 9 demethylases regulate self-renewal in embryonic stem cells. *Genes Dev.* 21, 2545–2557.
- Lu, R., Yang, A., and Jin, Y. (2011). Dual functions of T-box 3 (Tbx3) in the control of self-renewal and extraembryonic endoderm differentiation in mouse embryonic stem cells. *J. Biol. Chem.* 286, 8425–8436.
- MacArthur, B.D., and Lemischka, I.R. (2013). Statistical mechanics of pluripotency. *Cell* 154, 484–489.
- MacArthur, B.D., Sevilla, A., Lenz, M., Müller, F.J., Schuldt, B.M., Schuppert, A.A., Ridden, S.J., Stumpf, P.S., Fidalgo, M., Ma'ayan, A., et al. (2012). Nanog-dependent feedback loops regulate murine embryonic stem cell heterogeneity. *Nat. Cell Biol.* 14, 1139–1147.
- Marson, A., Foreman, R., Chevalier, B., Bilodeau, S., Kahn, M., Young, R.A., and Jaenisch, R. (2008a). Wnt signaling promotes reprogramming of somatic cells to pluripotency. *Cell Stem Cell* 3, 132–135.
- Marson, A., Levine, S.S., Cole, M.F., Frampton, G.M., Brambrink, T., Johnstone, S., Guenther, M.G., Johnston, W.K., Wernig, M., Newman, J., et al. (2008b). Connecting microRNA genes to the core transcriptional regulatory circuitry of embryonic stem cells. *Cell* 134, 521–533.
- Martin, G.R. (1981). Isolation of a pluripotent cell line from early mouse embryos cultured in medium conditioned by teratocarcinoma stem cells. *Proc. Natl. Acad. Sci. USA* 78, 7634–7638.
- Martin, B.L., and Kimelman, D. (2010). Brachyury establishes the embryonic mesodermal progenitor niche. *Genes Dev.* 24, 2778–2783.
- Mendjan, S., Mascetti, V.L., Ortmann, D., Ortiz, M., Karjosukarso, D.W., Ng, Y., Moreau, T., and Pedersen, R.A. (2014). NANOG and CDX2 pattern distinct subtypes of human mesoderm during exit from pluripotency. *Cell Stem Cell* 15, 310–325.
- Merrill, B.J. (2012). Wnt pathway regulation of embryonic stem cell self-renewal. *Cold Spring Harb. Perspect. Biol.* 4, a007971.
- Mullen, A.C., Orlando, D.A., Newman, J.J., Lovén, J., Kumar, R.M., Bilodeau, S., Reddy, J., Guenther, M.G., DeKoter, R.P., and Young, R.A. (2011). Master transcription factors determine cell-type-specific responses to TGF- $\beta$  signaling. *Cell* 147, 565–576.
- Murry, C.E., and Keller, G. (2008). Differentiation of embryonic stem cells to clinically relevant populations: lessons from embryonic development. *Cell* 132, 661–680.
- Narayanan, A., Thompson, S.A., Lee, J.J., and Lekven, A.C. (2011). A transgenic wnt8a:PAC reporter reveals biphasic regulation of vertebrate mesoderm development. *Dev. Dyn.* 240, 898–907.
- Niwa, H., Burdon, T., Chambers, I., and Smith, A. (1998). Self-renewal of pluripotent embryonic stem cells is mediated via activation of STAT3. *Genes Dev.* 12, 2048–2060.
- Niwa, H., Ogawa, K., Shimosato, D., and Adachi, K. (2009). A parallel circuit of LIF signalling pathways maintains pluripotency of mouse ES cells. *Nature* 460, 118–122.



- Nostro, M.C., Cheng, X., Keller, G.M., and Gadue, P. (2008). Wnt, activin, and BMP signaling regulate distinct stages in the developmental pathway from embryonic stem cells to blood. *Cell Stem Cell* 2, 60–71.
- Nusse, R., and Varmus, H. (2012). Three decades of Wnts: a personal perspective on how a scientific field developed. *EMBO J.* 31, 2670–2684.
- Ogawa, K., Nishinakamura, R., Iwamatsu, Y., Shimosato, D., and Niwa, H. (2006). Synergistic action of Wnt and LIF in maintaining pluripotency of mouse ES cells. *Biochem. Biophys. Res. Commun.* 343, 159–166.
- Pereira, C.F., and Fisher, A.G. (2009). Heterokaryon-based reprogramming for pluripotency. *Curr. Protoc. Stem Cell Biol. Chapter* 4, 4B.1.
- Price, F.D., Yin, H., Jones, A., van Ijcken, W., Grosveld, F., and Rudnicki, M.A. (2013). Canonical Wnt signaling induces a primitive endoderm metastable state in mouse embryonic stem cells. *Stem Cells* 31, 752–764.
- Renard, C.A., Labalette, C., Armengol, C., Cougot, D., Wei, Y., Cairo, S., Pineau, P., Neuveut, C., de Reyniès, A., Dejean, A., et al. (2007). *Tbx3* is a downstream target of the Wnt/beta-catenin pathway and a critical mediator of beta-catenin survival functions in liver cancer. *Cancer Res.* 67, 901–910.
- Rugg-Gunn, P.J., Cox, B.J., Ralston, A., and Rossant, J. (2010). Distinct histone modifications in stem cell lines and tissue lineages from the early mouse embryo. *Proc. Natl. Acad. Sci. USA* 107, 10783–10790.
- Sato, N., Meijer, L., Skaltsounis, L., Greengard, P., and Brivanlou, A.H. (2004). Maintenance of pluripotency in human and mouse embryonic stem cells through activation of Wnt signaling by a pharmacological GSK-3-specific inhibitor. *Nat. Med.* 10, 55–63.
- ten Berge, D., Kurek, D., Blauwkamp, T., Koole, W., Maas, A., Eroglu, E., Siu, R.K., and Nusse, R. (2011). Embryonic stem cells require Wnt proteins to prevent differentiation to epiblast stem cells. *Nat. Cell Biol.* 13, 1070–1075.
- Tesar, P.J., Chenoweth, J.G., Brook, F.A., Davies, T.J., Evans, E.P., Mack, D.L., Gardner, R.L., and McKay, R.D. (2007). New cell lines from mouse epiblast share defining features with human embryonic stem cells. *Nature* 448, 196–199.
- Thomson, M., Liu, S.J., Zou, L.N., Smith, Z., Meissner, A., and Ramathanan, S. (2011). Pluripotency factors in embryonic stem cells regulate differentiation into germ layers. *Cell* 145, 875–889.
- Tortelote, G.G., Hernández-Hernández, J.M., Quaresma, A.J., Nickerson, J.A., Imbalzano, A.N., and Rivera-Pérez, J.A. (2013). Wnt3 function in the epiblast is required for the maintenance but not the initiation of gastrulation in mice. *Dev. Biol.* 374, 164–173.
- Toyooka, Y., Shimosato, D., Murakami, K., Takahashi, K., and Niwa, H. (2008). Identification and characterization of subpopulations in undifferentiated ES cell culture. *Development* 135, 909–918.
- van Oosten, A.L., Costa, Y., Smith, A., and Silva, J.C. (2012). JAK/STAT3 signalling is sufficient and dominant over antagonistic cues for the establishment of naive pluripotency. *Nat Commun* 3, 817.
- Wang, J., Rao, S., Chu, J., Shen, X., Levasseur, D.N., Theunissen, T.W., and Orkin, S.H. (2006). A protein interaction network for pluripotency of embryonic stem cells. *Nature* 444, 364–368.
- Weidgang, C.E., Russell, R., Tata, P.R., Kühl, S.J., Illing, A., Müller, M., Lin, Q., Brunner, C., Boeckers, T.M., Bauer, K., et al. (2013). *TBX3* Directs Cell-Fate Decision toward Mesendoderm. *Stem Cell Rev.* 1, 248–265.
- Whyte, W.A., Orlando, D.A., Hnisz, D., Abraham, B.J., Lin, C.Y., Kagey, M.H., Rahl, P.B., Lee, T.I., and Young, R.A. (2013). Master transcription factors and mediator establish super-enhancers at key cell identity genes. *Cell* 153, 307–319.
- Yamaguchi, T.P., Takada, S., Yoshikawa, Y., Wu, N., and McMahon, A.P. (1999). T (Brachyury) is a direct target of Wnt3a during paraxial mesoderm specification. *Genes Dev.* 13, 3185–3190.
- Yamashita, J., Itoh, H., Hirashima, M., Ogawa, M., Nishikawa, S., Yurugi, T., Naito, M., Nakao, K., and Nishikawa, S. (2000). Flk1-positive cells derived from embryonic stem cells serve as vascular progenitors. *Nature* 408, 92–96.
- Yang, L., Cai, C.L., Lin, L., Qyang, Y., Chung, C., Monteiro, R.M., Mummery, C.L., Fishman, G.I., Cogen, A., and Evans, S. (2006). *Isl1*Cre reveals a common Bmp pathway in heart and limb development. *Development* 133, 1575–1585.
- Yasunaga, M., Tada, S., Torikai-Nishikawa, S., Nakano, Y., Okada, M., Jakt, L.M., Nishikawa, S., Chiba, T., Era, T., and Nishikawa, S. (2005). Induction and monitoring of definitive and visceral endoderm differentiation of mouse ES cells. *Nat. Biotechnol.* 23, 1542–1550.
- Yi, F., Pereira, L., Hoffman, J.A., Shy, B.R., Yuen, C.M., Liu, D.R., and Merrill, B.J. (2011). Opposing effects of Tcf3 and Tcf1 control Wnt stimulation of embryonic stem cell self-renewal. *Nat. Cell Biol.* 13, 762–770.
- Ying, Q.L., Wray, J., Nichols, J., Batlle-Morera, L., Doble, B., Woodgett, J., Cohen, P., and Smith, A. (2008). The ground state of embryonic stem cell self-renewal. *Nature* 453, 519–523.
- Zhang, X., Peterson, K.A., Liu, X.S., McMahon, A.P., and Ohba, S. (2013). Gene regulatory networks mediating canonical Wnt signal-directed control of pluripotency and differentiation in embryonic stem cells. *Stem Cells* 31, 2667–2679.

**Stem Cell Reports, Volume 5**

**Supplemental Information**

## **Tbx3 Controls Dppa3 Levels and Exit from Pluripotency toward Mesoderm**

**Avinash Waghray, Néstor Saiz, Anitha D. Jayaprakash, Ana G. Freire, Dmitri**

**Papatsenko, Carlos-Filipe Pereira, Dung-Fang Lee, Ran Brosh, Betty Chang, Henia Darr,**

**Julian Gingold, Kevin Kelley, Christoph Schaniel, Anna-Katerina Hadjantonakis, and**

**Ihor R. Lemischka**

## **Supplemental Information**

### **Tbx3 controls Dppa3 levels and exit from pluripotency towards mesoderm**

#### **SUPPLEMENTAL EXPERIMENTAL PROCEDURES**

##### **shRNA design and viral infection**

The lentiviral shRNA oligos were designed and constructed as described (Lee et al., 2012). Briefly, lentiviral particles were made by expressing the respective shRNA constructs along with pCMVΔ8.9 and pVSVG vectors in 293T cells. The supernatant was collected 72 hours after transfection and filtered through a 0.45μM sterile filters. The filtered supernatant was concentrated using Ultracel 30K ultra centrifuge filters at 3000rpm for 30 minutes as described (Lee et al., 2012). The concentrate along with 6μg/μl of polybrene was used to infect mESCs.

##### **Heterokaryon reprogramming assay**

The self-renewal ability of mESCs was assayed by fusing mESCs with human B cells as described (Lee et al., 2012a). Reprogramming of human ESCs was assayed by measuring mRNA expression of key genes, as needed using qRT-PCR (Pereira et al., 2008).

##### **Generation of Tbx3 targeting vector and Tbx3 null mESCs**

Tbx3 null mESCs were generated from Tbx3 heterozygote ( $Tbx3^{+/N}$ ) mESCs that have been described previously (Davenport et al., 2003). Tbx3 heterozygous cells ( $Tbx3^{+/N}$  cells) were kindly donated by Dr. V. E. Papaioannou from Columbia University Medical

Center.  $Tbx3^{N/N}$  mESCs were generated by culturing  $Tbx3^{+/N}$  cells in 2000  $\mu\text{g}/\mu\text{l}$  of genetecin in long-term cultures. Colonies were picked and analyzed for a normal karyotype. Karyotype of the  $Tbx3^{N/N}$  cells was assayed at the company “Cell line genetics”. To generate  $Tbx3^{N/P}$  cells the wild type allele in  $Tbx3^{+/N}$  cells was re-targeted by homologous recombination using a targeting vector. The targeting vector was generated using the pFlexible-puro vector (a kind gift from Jianlong Wang’s lab at Icahn School of Medicine at Mount Sinai). Two homologous arms were cloned into the PmeI/AsclI (5’) and NotI (3’) sites. The arms were PCR amplified from genomic DNA of R1 mESCs using primers listed in table S4. The targeting of drug selected  $Tbx3$  null mESCs ( $Tbx3^{N/N}$  and  $Tbx3^{N/P}$ ) was tested by genomic PCR (Table S4) and confirmed by Southern blotting as described (Carvajal-Vergara et al., 2010). T3Blast mESCs were derived from blastocyst stage embryos (E3.75), collected from  $Tbx3^{+/-}$  intercrosses, as previously described previously (Czechanski et al., 2014).

### **Derivation of blastocysts, immunofluorescence and image acquisition**

Blastocysts were collected at E3.75 or E4.5 from  $Tbx3^{+/-}$  females bred to  $Tbx3^{+/-}$  males (C57BL/6xCD1) (Davenport et al., 2003). The day of detection of vaginal plug was considered E0.5. Embryos were flushed from oviducts in FHM medium (Millipore) and fixed subsequently in 4% paraformaldehyde in PBS (Electron Microscopy Sciences).

Whenever necessary, zona pellucida was removed by brief incubation in acidic Tyrode’s solution (Sigma). Mice were maintained under a 12h light/dark cycle in the designated facilities of Memorial Sloan Kettering Cancer Center (MSKCC). Mouse work was subject

to approval by, and carried out in accordance with guidelines from MSKCC's Institutional Animal Care and Use Committee. Immunofluorescence (IF) was performed as described (Frankenberg et al., 2013). Imaging was carried out on a Zeiss LSM 510 META confocal microscope, using a Plan-Neofluar 40x/1.3 Oil DIC objective. Embryos were mounted in drops of 5µg/ml Hoechst 33342 solution (Life Technologies) and 1µm optical sections were acquired to build whole-embryo z-stacks. Images were segmented for cell counting using the MINS software (Lou et al., 2014) and data was processed as previously described (Schrode et al., 2014). Following imaging, embryos were lysed for genotyping as described previously (Kang et al., 2013). The primers used for both embryo and ES cell genotyping have been previously published (Davenport et al., 2003).

### **Generation of cell lines and cell culture conditions**

All mESCs were cultured in mESC media as described (Ang et al., 2011; Lee et al., 2012). Tbx3R rescue clones were described previously (Ivanova et al., 2006). Dppa3R and genetic complementation system cell lines was made by introducing the pLKO.1-pig based transgenic vector (Lee et al., 2012) along with empty pTRIPz vector (for rtTA3) into Tbx3<sup>+/+</sup> and Tbx3<sup>N/N</sup> cells in the presence of Dox. Tbx3<sup>N/N</sup>+Tbx3 Tg cell line was constructed by introducing a Dox inducible Tbx3 vector made by cloning Tbx3 cDNA into the pTRIPz vector (Table S4). Tbx3<sup>N/N</sup>+BirA cell line was generated by introducing the biotin ligase enzyme BirA cDNA into Tbx3<sup>N/N</sup> cells by electroporation as described (Wang et al., 2006). Tbx3<sup>N/N</sup>+BirA+bfTbx3 cell line was generated by introducing the Flag-Biotin tagged Tbx3 cDNA (Table S4) into Tbx3<sup>N/N</sup>+BirA cells. Tbx3i cell lines were generated

from the KH2 parental cell line (Beard et al., 2006). Tbx3 isoform2 was knocked into the ColA1 locus using the Flp-in expression vector pBS31'-RBGpA-Tbx3Iso2 generated using vectors from the Thermo scientific open biosystems targeting kit. Briefly,  $\sim 10^7$  cells were electroporated with 15 $\mu$ g each of the pBS31'-RBGpA-Tbx3Iso2 and pCAGGS-FLPe-puro vectors. Hygromycin (140  $\mu$ g/ml) was added into the media 24 hours after the electroporation. Surviving colonies were picked and positive clones were selected by qRT-PCR with and without Dox. Recombinant Wnt3a was used at the indicated concentrations. All cell culture reagents and chemicals mentioned above were purchased through the Pluripotent Stem Cell shared resource facility (SRF) at Mount Sinai (<http://icahn.mssm.edu/research/resources/shared-resource-facilities/human-embryonic-stem-cell>). Human ESCs were cultured in human ESC media on matrigel as described (Carvajal-Vergara et al., 2010). Human B cells used for heterokaryon-based reprogramming assay were cultured as described (Pereira et al., 2008).

### **Quantitative real-time (qRT) PCR analysis**

Analysis of mRNA expression by qRT-PCR analysis was done using the Fast SYBR green 2X master mix kit from Applied biosystems. The primers used are mentioned in table S4. The reactions were run on the Roche lightcycler 480 machine.

### **Western blotting and antibodies**

Western blotting was done as described (Lee et al., 2012). List of antibodies used are mentioned in table S4.

### **Alkaline phosphatase staining, FACS analysis and immunofluorescence**

Alkaline phosphatase (AP) staining was done following manufacturer's instructions using the Stemgent or Millipore kits as described (Lee et al., 2012). To test the colony forming ability of mESCs, single SSEA1+ mESCs were sorted on to 96 well plates (Flow Cytometry Core, Icahn School of Medicine at Mount Sinai) and emergence of AP positive colonies was scored. SSEA1 staining was done following manufacturer's instructions using the BD Pharmingen kit. Wild type cells stained with IgM-APC (Table S4) was used as negative control in figure 2K. IF on mESCs was done using the antibodies listed in table S4 as described (Carvajal-Vergara et al., 2010).

### **ChIP-Seq and mRNA-Seq Sample preparation**

ChIP-Seq sample preparation was performed as described (Ang et al., 2011). Briefly, cells were fixed with 11% formaldehyde in mESC media for 10 minutes on a rotating platform. The fixation was stopped by addition of 125nM of Glycine for 5 minutes on a rotating platform. Cells were scrapped, quick-frozen and stored at -80°C. ChIP was done by pulling down the bfTbx3 protein using Dynabeads conjugated to streptavidin (SA) from Tbx3<sup>N/N</sup>+NBirA+bfTbx3 cells. Pull down in Tbx3<sup>N/N</sup>+NBirA cells was used as negative control. DNA library preparation was done using the Illumina ChIP-seq sample prep kit. The libraries were run on HiSeq 2000 machines at the genomics SRF at Icahn school of medicine at Mount Sinai (<http://icahn.mssm.edu/departments-and-institutes/genomics/about/resources/genomics-core-facility>).

For mRNA-Seq sample preparation, the total RNA was isolated using Trizol reagent following the manufacturer's instructions. Quality and quantity of total RNA was assayed using Nanodrop and Agilent Bioanalyzer. Further, mRNA-seq libraries were prepared using the TrueSeq protocol from Illumina. Briefly, mRNA from 500ng-1 µg of total RNA was isolated using poly T beads. Double stranded cDNA was made using super-script reverse transcriptase and random primers. The cDNA ends were blunted, "A" base added and adapters ligated to each end of the cDNA. Total of 15 cycles of PCR were performed to generate the cDNA libraries. The concentration of the libraries was assayed using Agilent Bioanalyzer and sequenced either using 1\*26bp or 1\*100bp on an Illumina Genome analyzer II or HiSeq 2000 platform at the genomics SRF at Mount Sinai.

For single cell mRNA-Seq preparation, SSEA1+DAPI- mESCs were sorted and collected. The cDNA synthesis was done following the manufacturers instruction using the C1 Single-Cell Auto Prep System (Fluidigm). Amount of cDNA synthesized was quantified using the Quant-iT™ PicoGreen® dsDNA Assay Kit (Life Technologies). Sequencing libraries were prepared using the Nextera XT DNA Library Prep Kit (Illumina). About 24 libraries were mixed together. The concentration of the mixed libraries was assayed using Agilent Bioanalyzer. The libraries were sequenced using 1\*100bp on a HiSeq 2000/2500 platform at the genomics SRF at Mount Sinai and NYU genomics core.

### **Next-Gen sequencing analysis and other analyses**

ChIP-Seq analysis was done on the raw Fastq files received. The fastq files were mapped to the mouse mm9 genome using Bowtie (v1.0) program allowing for 2 base pair

mismatches. The mapped output file was processed through MACS analysis (v1.4) software to determine peaks. Homer software package (<http://homer.salk.edu/homer/index.html>) was used for annotation of the peaks and further analysis was carried out using the R statistical software. The bigWig files were generated using the Galaxy server (<https://usegalaxy.org>). The ChIP dataset for  $\beta$ -catenin was annotated from literature (Zhang et al., 2013).  $\beta$ -catenin bound regions are determined as those regions bound in both Flag and Biotin ChIP pull downs in the samples with induction of Wnt signaling. The UCSC genome browser was used to visualize the bigWig files from ChIP-Seq datasets.

For mRNA-Seq analysis the raw fastq files were mapped to the mouse mm9 genome using Tophat (with bowtie2). The output files were processed through Cufflinks and Cuffdiff programs to conduct differential gene expression analysis. The output “.bam” files from Tophat were used to generate the bedGraph files using Homer software package. Briefly, within the homer package “.bam” files were used to generate tagdirectories using makeTagDirectory command. The tagdirectories were then used to generate bedGraph files using the makeUCSCfile command. The UCSC genome browser was used to visualize the bedGraph files from mRNA-Seq datasets. CummeRbund was used as needed for analysis of the raw Fastq files and the output files from Cuffdiff program.

For single cell mRNA-Seq analysis the raw fastq files were mapped to the mouse mm9 genome using Tophat (with bowtie2). The output “.bam” files were processed through

Cuffquant program. The output “.cxb” files from Cuffquant were processed through Cuffnorm program to generate FPKM values. The p value for the anti-correlation of expression between Tbx3 and Dppa3 in cells expressing these TFs was calculated using Student t-distribution test.

R software was used to do the statistics as needed. Quantile analysis was done by calculating the Q-scores to rank the genes as described previously (Creyghton et al., 2010). The distribution of quantile scores was plotted as bar plots and the significance between the different datasets was calculated by Wilcoxon rank sum test with continuity correction using the R statistical software. For both ChIP-Seq and mRNA-Seq analysis the mm9 mouse reference genome used.

Microarray data used to generate the correlation plots in Figure 2A and 2B was from published data (Hailesellasse Sene et al., 2007). Microarray data used to generate the data in Figure S3B and S4E was from published literature (Mikkelsen et al., 2008). Gene set enrichment analysis (GSEA) was performed following standard instructions from the standalone java tool downloaded from [www.broadinstitute.org/gsea](http://www.broadinstitute.org/gsea). FPKM values were used to make the pre ranked lists. The gene sets were annotated from Amigo gene ontology terms and are available on request.

## SUPPLEMENTAL REFERENCES

- Ang, Y.S., Tsai, S.Y., Lee, D.F., Monk, J., Su, J., Ratnakumar, K., Ding, J., Ge, Y., Darr, H., Chang, B., *et al.* (2011). Wdr5 mediates self-renewal and reprogramming via the embryonic stem cell core transcriptional network. *Cell* *145*, 183-197.
- Beard, C., Hochedlinger, K., Plath, K., Wutz, A., and Jaenisch, R. (2006). Efficient method to generate single-copy transgenic mice by site-specific integration in embryonic stem cells. *Genesis* *44*, 23-28.
- Carvajal-Vergara, X., Sevilla, A., D'Souza, S.L., Ang, Y.S., Schaniuel, C., Lee, D.F., Yang, L., Kaplan, A.D., Adler, E.D., Rozov, R., *et al.* (2010). Patient-specific induced pluripotent stem-cell-derived models of LEOPARD syndrome. *Nature* *465*, 808-812.
- Creyghton, M.P., Cheng, A.W., Welstead, G.G., Kooistra, T., Carey, B.W., Steine, E.J., Hanna, J., Lodato, M.A., Frampton, G.M., Sharp, P.A., *et al.* (2010). Histone H3K27ac separates active from poised enhancers and predicts developmental state. *Proceedings of the National Academy of Sciences of the United States of America* *107*, 21931-21936.
- Czechanski, A., Byers, C., Greenstein, I., Schrode, N., Donahue, L.R., Hadjantonakis, A.K., and Reinholdt, L.G. (2014). Derivation and characterization of mouse embryonic stem cells from permissive and nonpermissive strains. *Nature protocols* *9*, 559-574.
- Davenport, T.G., Jerome-Majewska, L.A., and Papaioannou, V.E. (2003). Mammary gland, limb and yolk sac defects in mice lacking *Tbx3*, the gene mutated in human ulnar mammary syndrome. *Development (Cambridge, England)* *130*, 2263-2273.
- Frankenberg, S., Shaw, G., Freyer, C., Pask, A.J., and Renfree, M.B. (2013). Early cell lineage specification in a marsupial: a case for diverse mechanisms among mammals. *Development* *140*, 965-975.
- Hailesellasse Sene, K., Porter, C.J., Palidwor, G., Perez-Iratxeta, C., Muro, E.M., Campbell, P.A., Rudnicki, M.A., and Andrade-Navarro, M.A. (2007). Gene function in early mouse embryonic stem cell differentiation. *BMC genomics* *8*, 85.
- Ivanova, N., Dobrin, R., Lu, R., Kotenko, I., Levorse, J., DeCoste, C., Schafer, X., Lun, Y., and Lemischka, I.R. (2006). Dissecting self-renewal in stem cells with RNA interference. *Nature* *442*, 533-538.
- Kang, M., Piliszek, A., Artus, J., and Hadjantonakis, A.K. (2013). FGF4 is required for lineage restriction and salt-and-pepper distribution of primitive endoderm factors but not their initial expression in the mouse. *Development* *140*, 267-279.
- Lee, D.F., Su, J., Ang, Y.S., Carvajal-Vergara, X., Mulero-Navarro, S., Pereira, C.F., Gingold, J., Wang, H.L., Zhao, R., Sevilla, A., *et al.* (2012). Regulation of embryonic and induced pluripotency by aurora kinase-p53 signaling. *Cell stem cell* *11*, 179-194.
- Lou, X., Kang, M., Xenopoulos, P., Munoz-Descalzo, S., and Hadjantonakis, A.K. (2014). A Rapid and Efficient 2D/3D Nuclear Segmentation Method for Analysis of Early Mouse Embryo and Stem Cell Image Data. *Stem Cell Reports* *2*, 382-397.
- Mikkelsen, T.S., Hanna, J., Zhang, X., Ku, M., Wernig, M., Schorderet, P., Bernstein, B.E., Jaenisch, R., Lander, E.S., and Meissner, A. (2008). Dissecting direct reprogramming through integrative genomic analysis. *Nature* *454*, 49-55.
- Pereira, C.F., Terranova, R., Ryan, N.K., Santos, J., Morris, K.J., Cui, W., Merckenschlager, M., and Fisher, A.G. (2008). Heterokaryon-based reprogramming of human B lymphocytes for pluripotency requires Oct4 but not Sox2. *PLoS genetics* *4*, e1000170.

Schrode, N., Saiz, N., Di Talia, S., and Hadjantonakis, A.K. (2014). GATA6 levels modulate primitive endoderm cell fate choice and timing in the mouse blastocyst. *Developmental cell* 29, 454-467.

Wang, J., Rao, S., Chu, J., Shen, X., Levasseur, D.N., Theunissen, T.W., and Orkin, S.H. (2006). A protein interaction network for pluripotency of embryonic stem cells. *Nature* 444, 364-368.

Zhang, X., Peterson, K.A., Liu, X.S., McMahon, A.P., and Ohba, S. (2013). Gene Regulatory Networks Mediating Canonical Wnt Signal Directed Control of Pluripotency and Differentiation in Embryo Stem Cells. *Stem cells*.

## SUPPLEMENTAL TABLES

**Table S1. Related to Figures 2 and 5.** mRNA-Seq data from Tbx3<sup>+/+</sup>, Tbx3<sup>+<sup>/</sup>N</sup>, Tbx3<sup>N/N</sup>, shLuc and shTbx3 containing mESCs.

**Table S2. Related to Figures 2 and 5.** ChIP-Seq targets of Tbx3 in mESCs

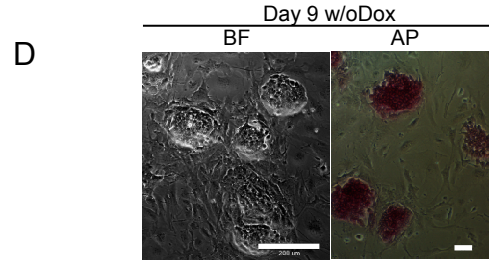
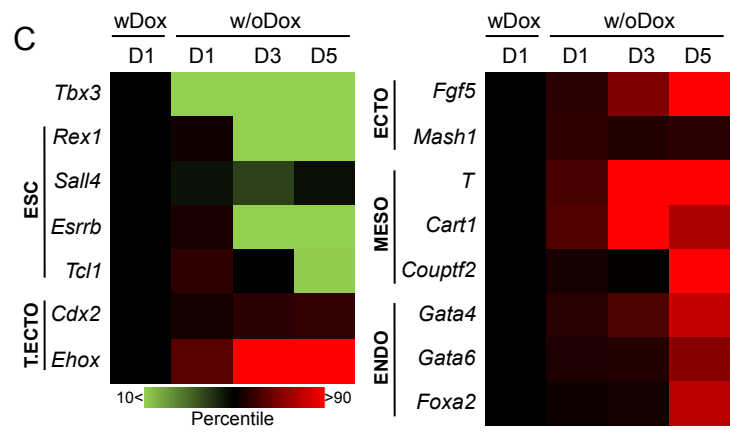
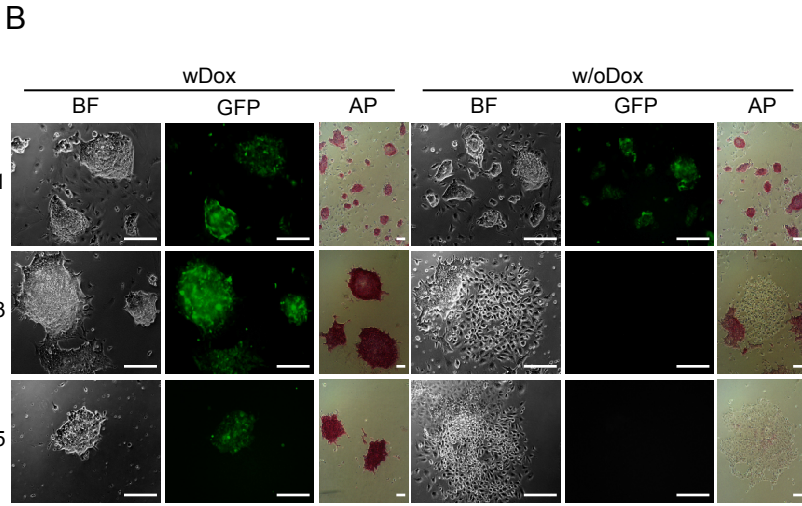
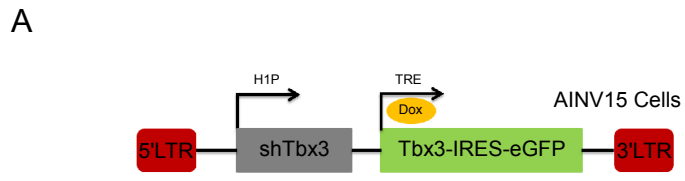
**Table S3. Related to Figures 3.** Single cell mRNA-Seq data of wild type R1 mESCs

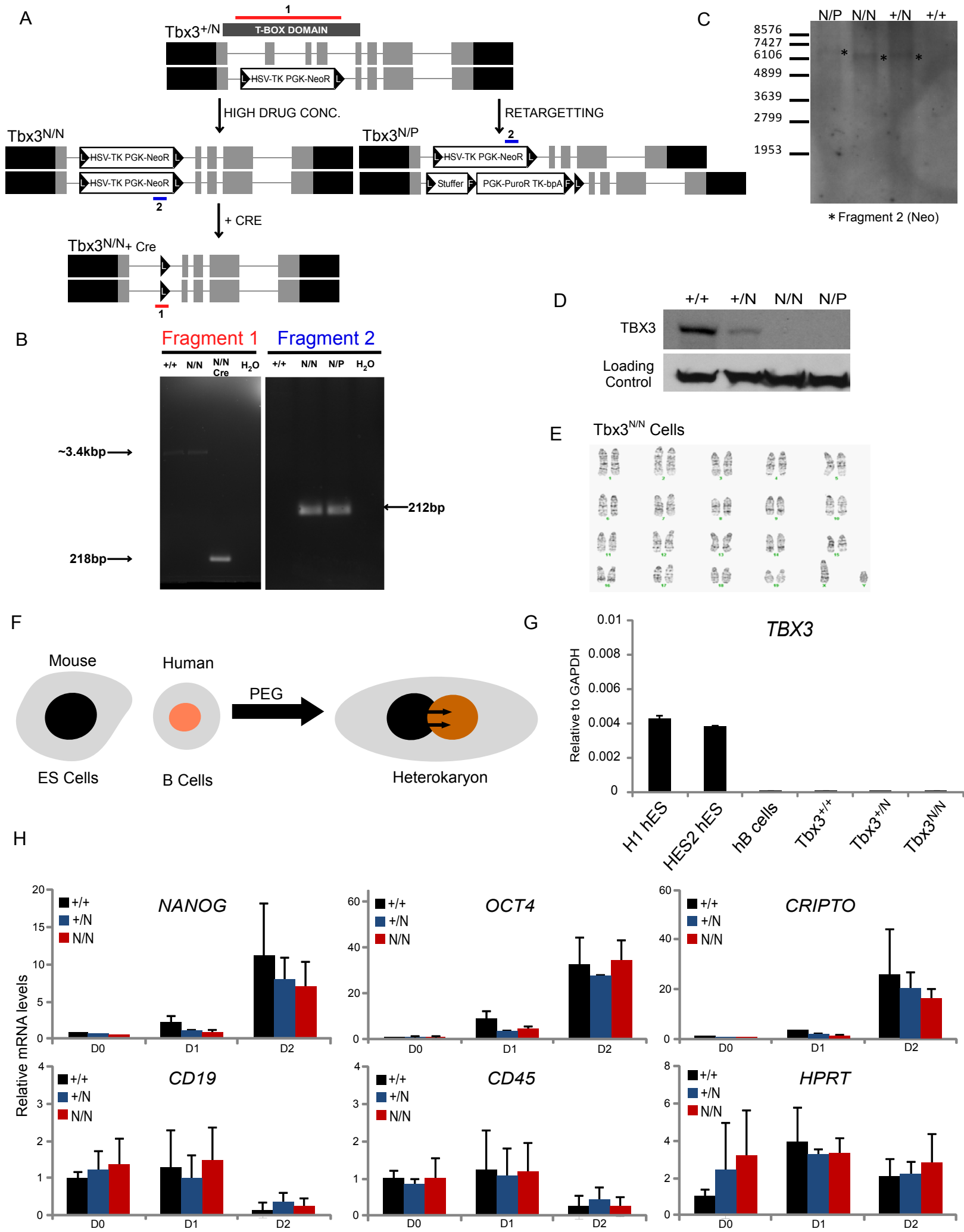
**Table S4. Related to all figures.** Oligos and antibodies used in the study.

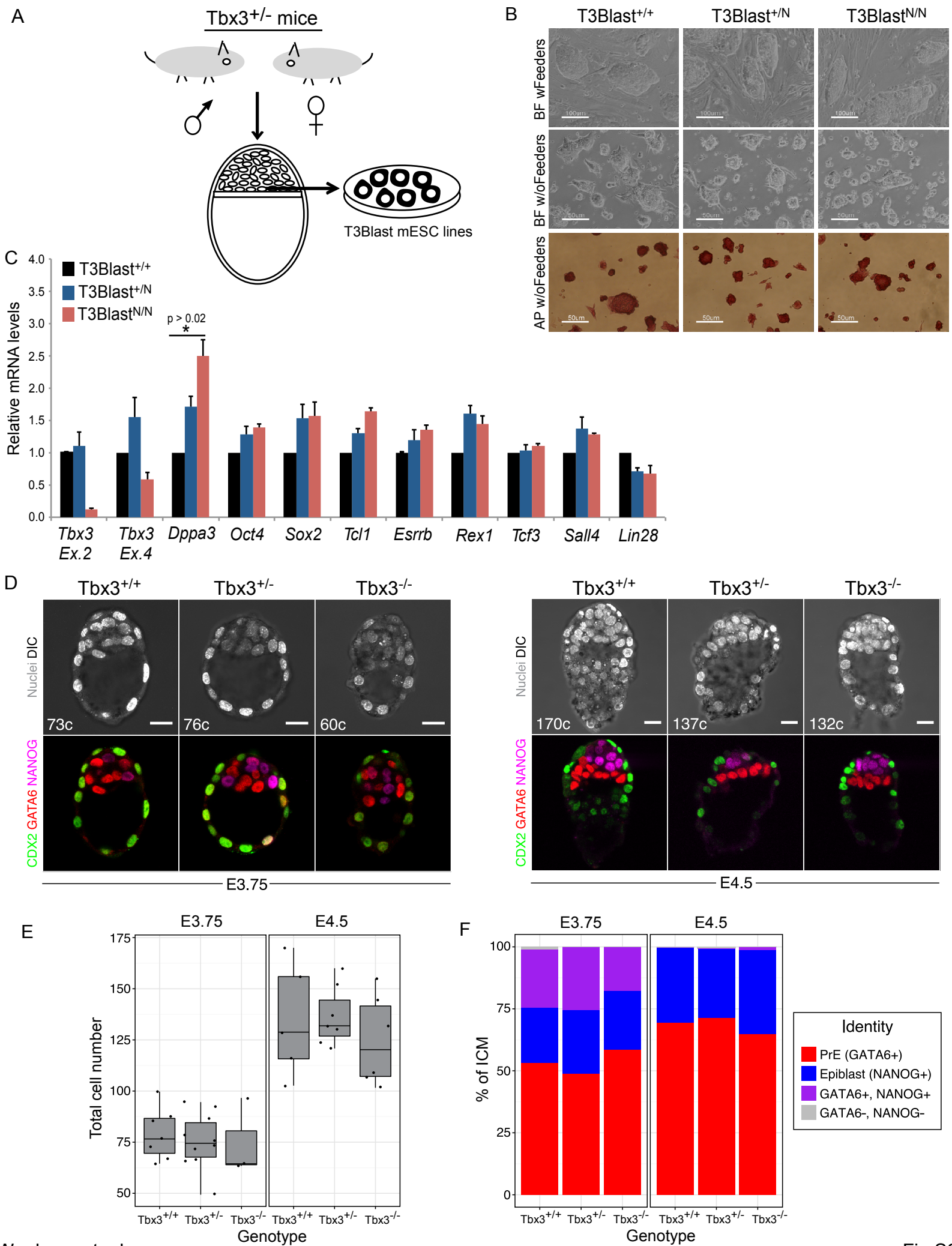
**Table S5. Related to Figure 2.** T3blast mESC lines and embryo counts

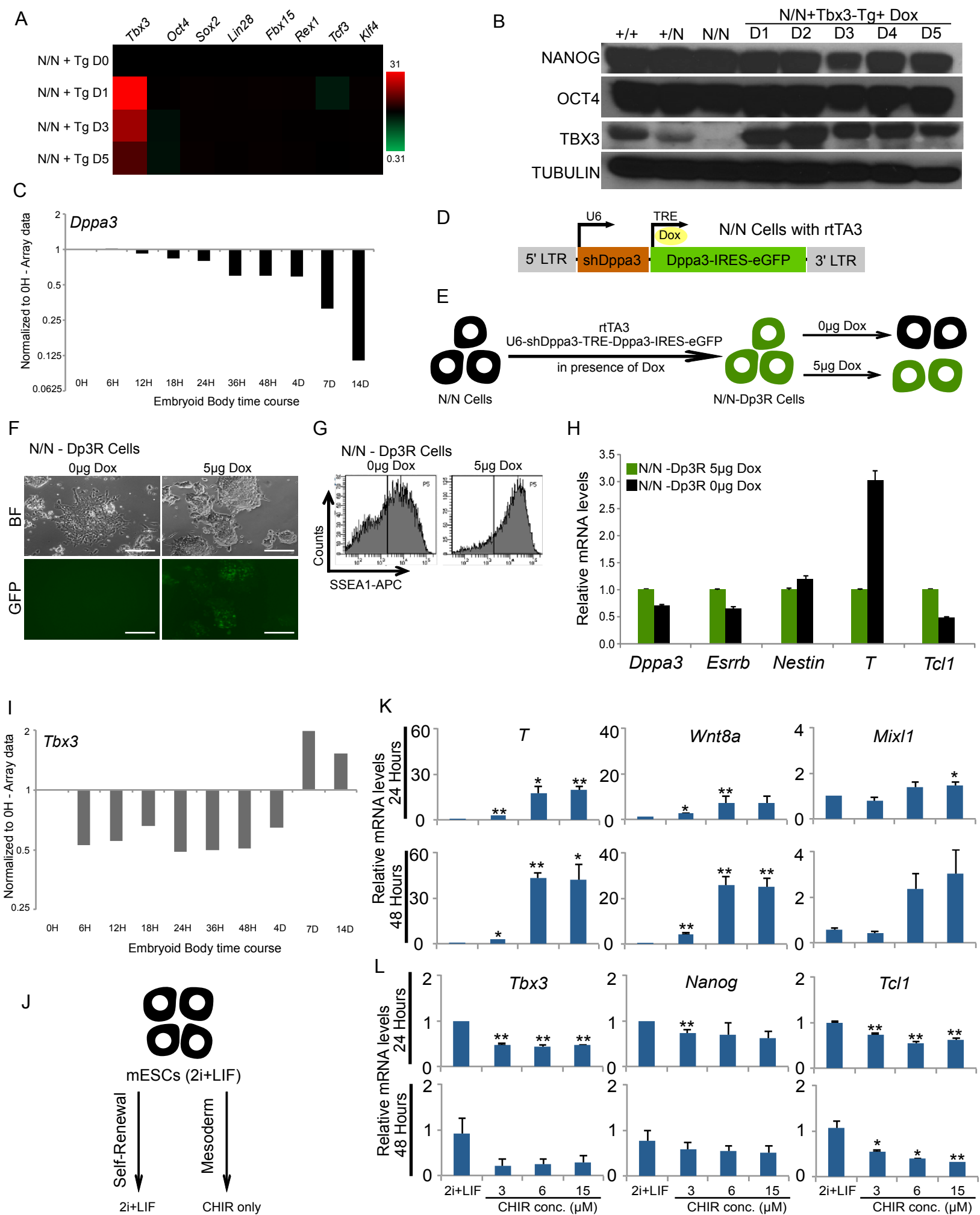
**Table S6. Related to Figure 2.** Number of E10.5 chimeric embryos

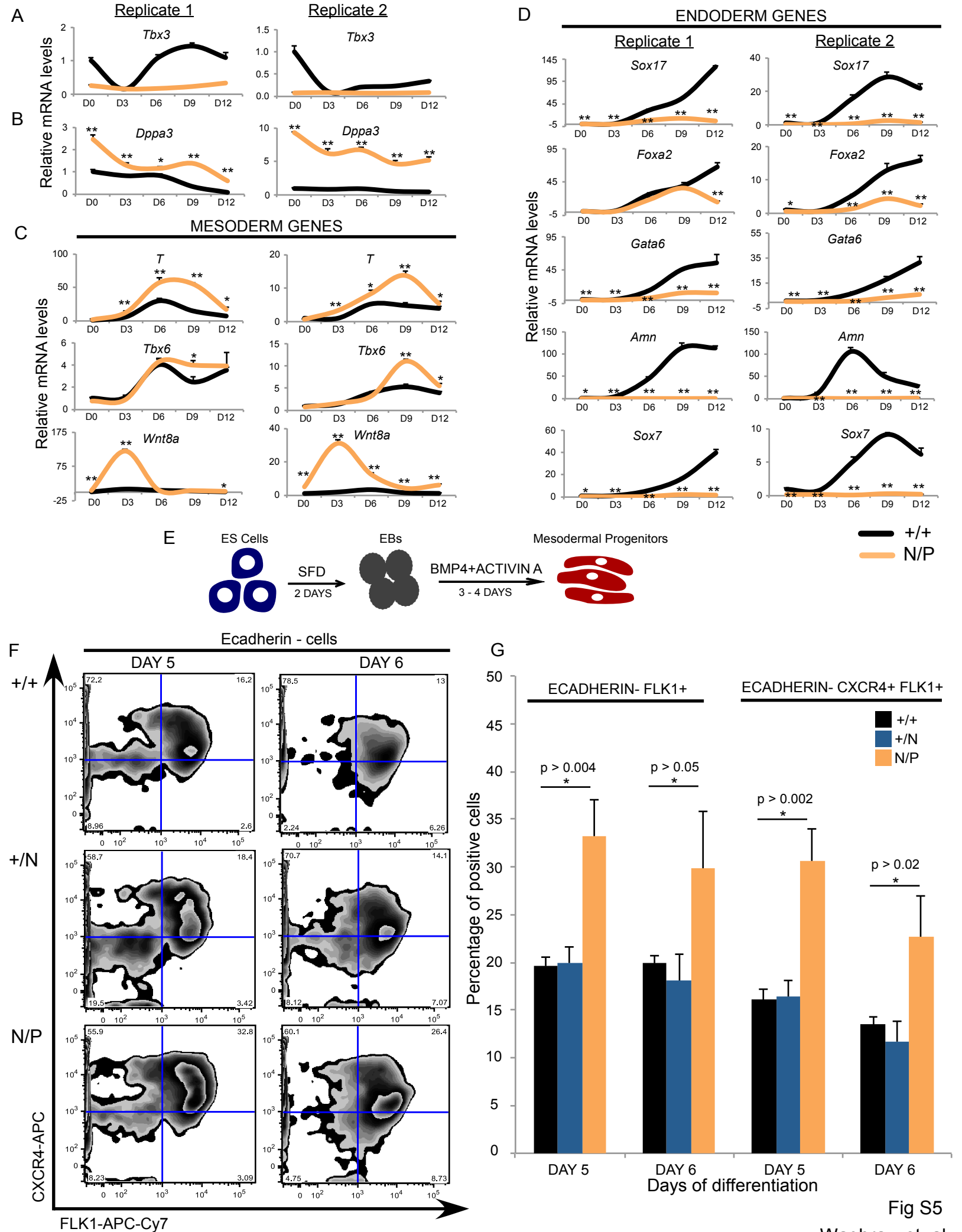
	+/N cells	N/N cells	N/P cells
No. of Blastocyst Injections	1	2	1
# of Chimeric* embryos (Total # of Embryos)	4(8)	11(12)	3(9)
* embryos with eGFP OR tdTomato expression			





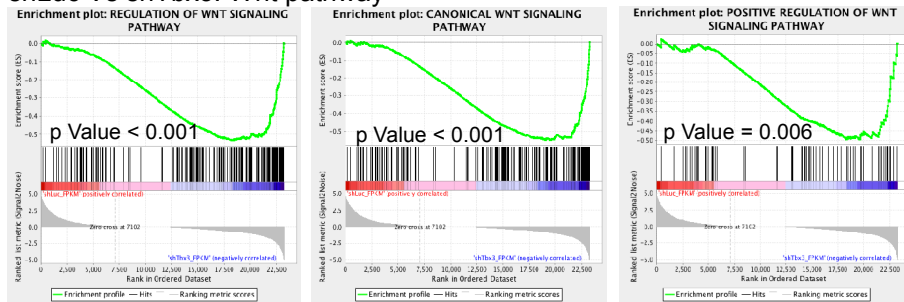




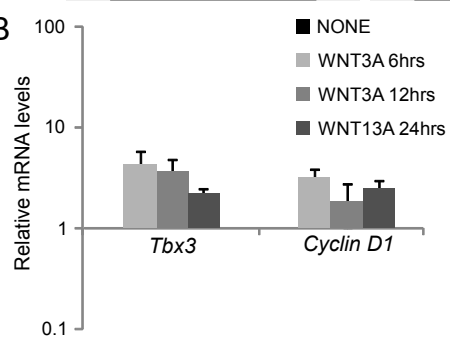


# shLuc Vs shTbx3: Wnt pathway

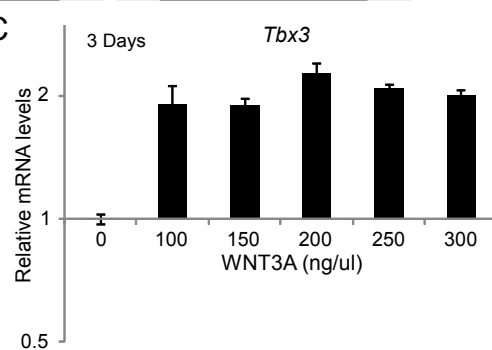
**A**



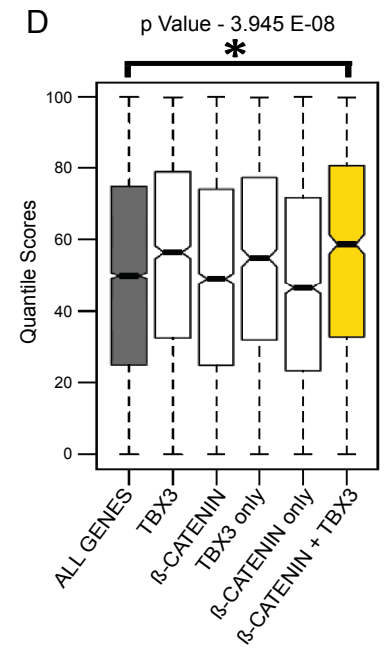
**B**



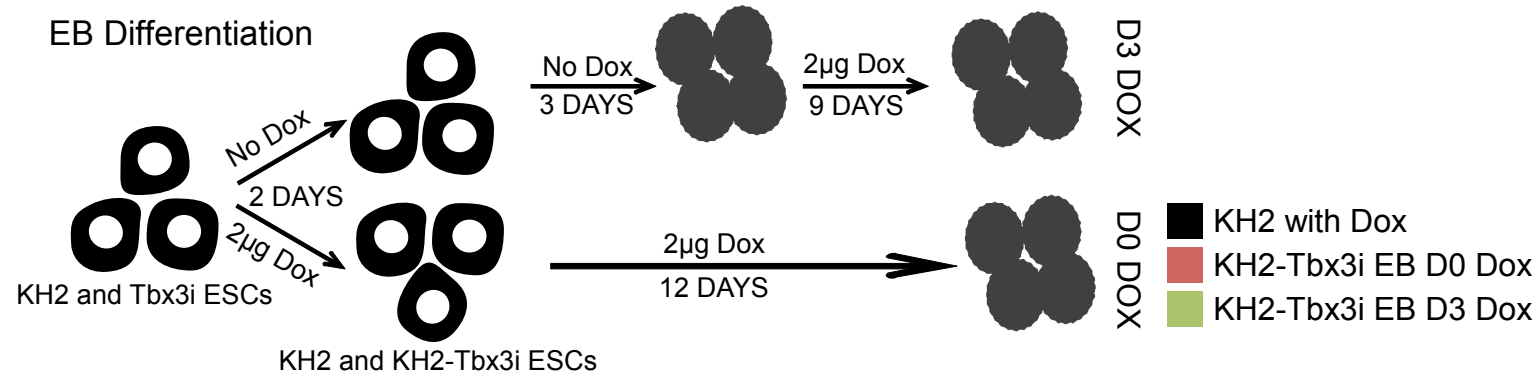
**C**



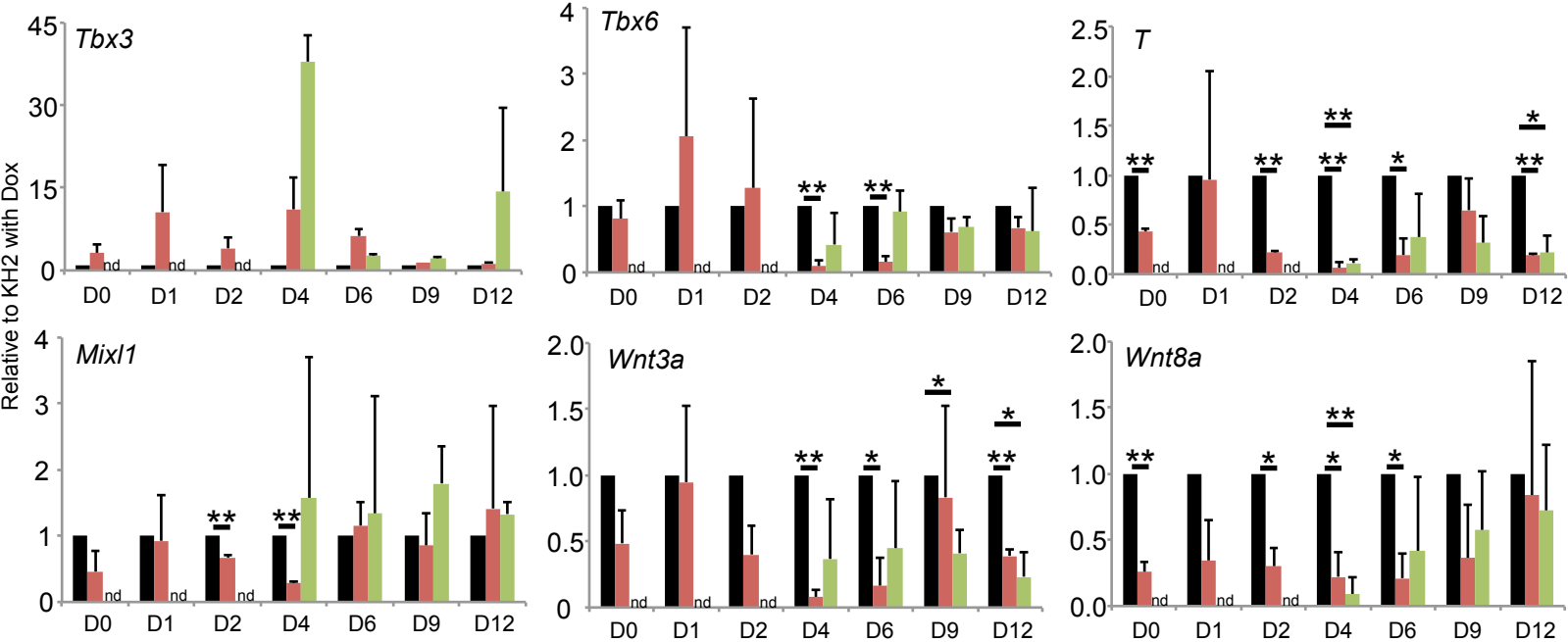
**D**



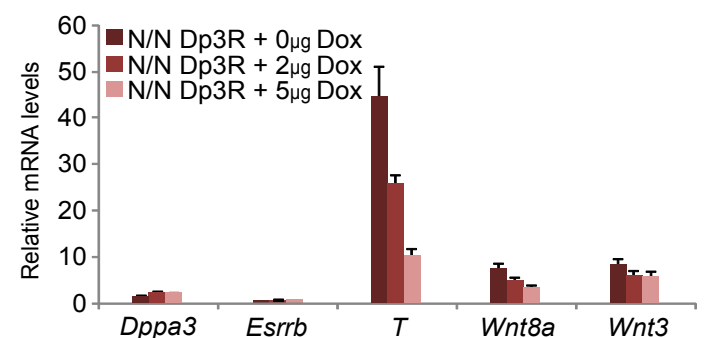
**E**



**F**



**G**



## SUPPLEMENTAL FIGURE LEGENDS

**Figure S1. Related to Figure 1. Tbx3 knock down in mESCs. A.** The construct used to control Tbx3 levels in Tbx3R cell line. **B.** Short-hairpin (sh)RNA mediated knock down of Tbx3 (w/o Dox) in mESCs causes morphological changes and loss of alkaline phosphatase (AP) staining. Endogenous Tbx3 is knocked down using a constitutively expressed shRNA and is replaced by a Dox-inducible shRNA immune exogenous Tbx3-IRES-eGFP cassette. Tbx3 levels in this system (Tbx3R) are therefore controlled by Dox addition. GFP levels represent expression of inducible Tbx3 transgene. Cells are maintained long term in the presence of Dox (Tbx3) in ESC media containing LIF. Effect of Tbx3 knockdown is assayed 1 day (D1), 3 days (D3) or 5 days (D5) after removal of Dox. **C.** mRNA expression levels of the indicated genes after the knockdown of Tbx3 using the Tbx3R cell line using qRT-PCR. The symbols indicate: ESC- ESC marker, T.ECTO- trophectodermal marker, ECTO- ectodermal marker, MESO- mesodermal marker and ENDO- endodermal markers **D.** Tbx3R cells are grown on gelatin in the absence of Doxycycline (Dox) for 9 days in ESC media containing LIF. Bright field (BF) and AP staining colony pictures are shown.

**Figure S2. Related to Figure 2. *In vitro* derived Tbx3 null mESCs. A.** Targeting strategy showing the genomic region of Tbx3 that was deleted. Also shown are the locations of the primers used to confirm the targeting. Cre recombinase enzyme was used to delete the neomycin cassette prior to use in blastocyst injection assay in Figure 1G. **B.** Genomic PCR for the indicated fragments to confirm targeting of Tbx3 null mESCs. Fragment 1 spans the deleted region. Fragment 2 amplifies with the neomycin cassette. The 3.4kbp

band from fragment 1 PCR indicates the size of the PCR product prior to deletion of neomycin cassette. **C.** Southern Blotting result using the probe for fragment 2, present in the neomycin cassette. The asterix (\*) indicates the position of positive bands. **D.** Level of Tbx3 protein measured by Western blot in indicated cell lines grown in ESC media containing LIF. Non-specific bands are used as loading control. **E.** Karyotype of Tbx3<sup>N/N</sup> mESCs grown in ESC media containing LIF. **F.** Schematic of the heterokaryon reprogramming assay. **G.** Tbx3 mRNA expression using a human TBX3 specific primer in H1 human (h)ESCs, HES2 hESCs, human B (hB) cells, Tbx3<sup>+/+</sup> cells, Tbx3<sup>+<sup>N</sup></sup> cells and Tbx3<sup>N/N</sup> cells. **H.** mRNA levels of indicated genes over a 2 days after heterokaryon-based reprogramming. NANOG, OCT4 and CRIPTO are used here as ESC markers. CD19 and CD45 are used as B cell markers. HPRT acts as housekeeping gene. Data represents average of three replicates.

**Figure S3. Related to Figure 2. Blastocyst derived Tbx3 null mESCs.** **A.** Schematic of Tbx3<sup>+/-</sup> mice and derivation of T3Blast mESCs. **B.** BF pictures of blastocyst derived T3Blast mESCs grown with (upper row) and without (middle row) feeders. AP staining colony pictures blastocyst derived T3Blast mESCs grown without feeders (lower row). **C.** mRNA levels of indicated ESC markers in mESCs cultured without feeders in the presence of LIF by qRT-PCR. Data is average of two replicates. The p values were generated using the t-test. **D.** Immunofluorescence for representative Tbx3<sup>+/+</sup>, Tbx3<sup>+/-</sup> and Tbx3<sup>-/-</sup> embryos at mid blastocyst (E3.75, left panels) and peri-implantation (E4.5, right panels) stages. CDX2 marks the trophectoderm lineage, GATA6 marks the primitive endoderm (PrE) and NANOG marks the epiblast. Total cell number for each embryo is shown on bright field

Waghray, et. al.

images. Scale bars = 20 $\mu$ m. **E.** Box plots showing total cell numbers for all embryos analyzed for each genotype and stage. Each spot represents one single embryo. **F.** Average ICM composition for each genotype and stage, shown as percentage of total ICM cells.

**Figure S4. Related to Figure 3. Tbx3 and Dppa3 during mESC differentiation. A.** mRNA levels of indicated genes in the Tbx3<sup>N/N</sup> +Tg cells grown in ESC media containing LIF and Dox (2 $\mu$ g/ml) **B.** Level of indicated proteins in Tbx3<sup>+/+</sup>, Tbx3<sup>+/N</sup>, Tbx3<sup>N/N</sup> and Tbx3<sup>N/N</sup> +Tg+Dox cells grown in ESC media containing LIF and Dox (2 $\mu$ g/ml). **C.** mRNA expression pattern of Dppa3 during the EB differentiation time course from published microarray data. **D.** Construct used to generate Tbx3<sup>N/N</sup>-Dp3R cell line from Tbx3<sup>N/N</sup> cells. **E.** Schematic explaining the strategy for generation of Tbx3<sup>N/N</sup>-Dp3R cells from Tbx3<sup>N/N</sup> cells followed by removal of Dox (0 $\mu$ g/ml) to knock down Dppa3 in Tbx3<sup>N/N</sup>-Dp3R cells. **F.** Morphology and GFP expression in Tbx3<sup>N/N</sup> (Tbx3<sup>N/N</sup>-Dp3R) mESCs harboring a Dppa3 genetic complementation system (Dp3R). When these cells are treated with Dox, a Dppa3 transgene compensates for Dppa3 knockdown. GFP reports the levels of transgene expression. To deliver rtTA3, cells were co-infected with an empty pTRIPz vector. **G.** Flow cytometry (FACS) analysis checking levels of SSEA1 protein in Tbx3<sup>N/N</sup>-Dp3R mESCs 7 days after removal of Dox. **H** mRNA levels of indicated genes 7 days after removal of Dox in Tbx3<sup>N/N</sup>-Dp3R cells using qRT-PCR. **I.** mRNA expression pattern Tbx3 during the EB differentiation time course from published microarray data. **G.** Schematic showing set up of experiment for Wnt mediated serum free differentiation into mesoderm lineage. **H-I.** mRNA expression levels of genes during the two day time

Waghray, et. al.

course of serum free differentiation. Data is average of two replicates. The p values were generated using the t-test. \* p value<0.05 and \*\* p value < 0.01.

**Figure S5. Related to Figure 4. *In vitro* differentiation potential of Tbx3 null mESCs. A-D.**

The mRNA expression pattern Tbx3 (A) and Dppa3 (B) genes, mesoderm genes (C) and endoderm genes (D) during the 12-day EB differentiation time course of Tbx3<sup>+/+</sup> and Tbx3<sup>N/P</sup> cells. Data from two independent replicates is shown. The p values were generated using the t-test. \* p value<0.05 and \*\* p value < 0.005. E. Schematic of serum free differentiation of mESCs into mesodermal progenitors. F. FACS plots displaying levels of CXCR4-APC and FLK1-APC-Cy7 in ECADHERIN-FITC negative cells on Day 5 and Day 6 time points during SFD. G. Quantification of the data in section F. FACS data is an average of three independent replicates. The p values were generated using the t-test.

**Figure S6. Related to Figure 5. Function of Tbx3 and Wnt signaling in maintenance of mESCs. A.** Gene set enrichment analysis to detect statistically significant gene sets in the given datasets. The panels show enrichment of the listed Wnt related gene ontology terms in the given datasets. **B.** Tbx3 mRNA expression in mESCs grown in ESC media containing LIF after a few hours of treatment with Wnt3a. **C.** Tbx3 mRNA expression in mESCs grown in ESC media containing LIF after 3 days of WNT3A treatment at indicated concentrations. **D.** mRNA expression profile from normalized mRNA-Seq dataset from wild type R1 mESCs. The expression data is represented as quantile scores, described in supplemental methods. The different datasets indicated here are: ALL GENES –All genes in the mRNA-Seq dataset; Tbx3 –TBX3 bound genes from ChIP-Seq study;  $\beta$ -catenin -  $\beta$ -

CATENIN bound genes from CHIP-Seq study; Tbx3 only – TBX3 bound genes not bound by  $\beta$ -CATENIN from CHIP-Seq studies;  $\beta$ -catenin only -  $\beta$ - CATENIN bound genes not bound by TBX3 from CHIP-Seq studies;  $\beta$ -catenin+Tbx3 – TBX3 and  $\beta$ - CATENIN co-bound genes. P-Value is calculated using the Wilcoxon rank sum test with continuity correction.

**E.** Schematic showing differentiation of KH2 and KH2-Tbx3i mESC lines as EBs. Dox (2 $\mu$ g/ml) is used to induce over expression of Tbx3. Tbx3 is over expressed either prior to differentiation (lower part) or after 3 days of differentiation (upper part). The parental KH2 line is used as control. **F.** mRNA Levels of Tbx3 and mesodermal markers during the EB differentiation process measured by qRT-PCR. Data represents average of two replicates. The p values were generated using the t-test. \* p value<0.05 and \*\* p value < 0.005. **G.** mRNA levels of indicated genes in Tbx3<sup>N/N</sup> cells after removal of Dox (knock down of *Dppa3*).